



A four-gene operon in *Bacillus cereus* produces two rare spore-decorating sugars

Received for publication, January 19, 2017 and in revised form, March 14, 2017 Published, Papers in Press, March 15, 2017, DOI 10.1074/jbc.M117.777417

Zi Li^{‡§}, Thiya Mukherjee[‡], Kyle Bowler[‡], Sholeh Namdari[‡], Zachary Snow[‡], Sarah Prestridge[‡], Alexandra Carlton[‡], and Maor Bar-Peled^{‡§1}

From the [‡]Complex Carbohydrate Research Center and the [§]Department of Plant Biology, University of Georgia, Athens, Georgia 30602

Edited by Chris Whitfield

Bacterial glycan structures on cell surfaces are critical for cell-cell recognition and adhesion and in host-pathogen interactions. Accordingly, unraveling the sugar composition of bacterial cell surfaces can shed light on bacterial growth and pathogenesis. Here, we found that two rare sugars with a 3-*C*-methyl-6-deoxyhexose structure were linked to spore glycans in *Bacillus cereus* ATCC 14579 and ATCC 10876. Moreover, we identified a four-gene operon in *B. cereus* ATCC 14579 that encodes proteins with the following sequential enzyme activities as determined by mass spectrometry and one- and two-dimensional NMR methods: CTP:glucose-1-phosphate cytidyltransferase, CDP-Glc 4,6-dehydratase, NADH-dependent SAM: C-methyltransferase, and NADPH-dependent CDP-3-*C*-methyl-6-deoxyhexose 4-reductase. The last enzyme predominantly yielded CDP-3-*C*-methyl-6-deoxyglucose (CDP-cereose) and likely generated a 4-epimer CDP-3-*C*-methyl-6-deoxyallose (CDP-cillose). Some members of the *B. cereus sensu lato* group produce CDP-3-*C*-methyl-6-deoxy sugars for the formation of cereose-containing glycans on spores, whereas others such as *Bacillus anthracis* do not. Gene knockouts of the *Bacillus* C-methyltransferase and the 4-reductase confirmed their involvement in the formation of cereose-containing glycan on *B. cereus* spores. We also found that cereose represented 0.2–1% spore dry weight. Moreover, mutants lacking cereose germinated faster than the wild type, yet the mutants exhibited no changes in sporulation or spore resistance to heat. The findings reported here may provide new insights into the roles of the uncommon 3-*C*-methyl-6-deoxy sugars in cell-surface recognition and host-pathogen interactions of the genus *Bacillus*.

Bacterial cells produce myriad glycan structures that are secreted or attached to cell surfaces. Often, being at the outermost surface of the cells, glycans have significant impact on cell-cell recognition, cell-to-cell adhesion, and host-pathogen

interactions (1–4). Glycans also play a profound role in shaping the cell (5). In recent years it has also been recognized that spore-producing bacteria like members of the *Bacillus cereus sensu lato* group are decorated with glycan structures (6, 7). Although very few of these glycans have been studied, they are found as glycoproteins of the spore exosporium, the outermost surface layer surrounding the spore coat. Among the exosporium glycoproteins that have been characterized are ExsH and the collagen-like protein BclA (8, 9). The BclA protein plays a central role in *Bacillus anthracis* pathogenesis by promoting the interaction of spores with the host phagocytic cell. This is proposed to facilitate transport of the spores to sites of spore germination and bacterial outgrowth (10, 11). These two glycoproteins characterized in the *B. cereus* ATCC 14579 exosporium have different sugar composition and glycosylation patterns (12). The reason for the presence of several surface glycoproteins differently glycosylated on *B. cereus* ATCC 14579 exosporium remains unknown, but various glycosylation patterns suggest specific recognition of different cell receptors.

Genome sequence analyses have revealed the presence of at least 13 different collagen-like protein-encoding genes, and proteomic studies indicate that some of them are in the exosporium (13). Whether these are also glycoproteins with glycans that differ in their sugar composition and sequence remains unknown. This is a critical feature for study because spore glycoepitopes may explain host recognition and strain specificity. Thus, using a systematic screen to identify sugar-containing polymers in spores, we have identified by GS-MS analyses new unknown sugar-like residues in spore glycans.

Here we have provided the evidence of two rare sugars, 3-*C*-methyl-6-deoxyhexoses, displayed on *Bacillus* spores. We show that the activated forms of the sugars are CDP-3-*C*-methyl-6-deoxyhexose isomers, as illustrated in Fig. 1. The formation of the *C*-methyl-sugar-containing glycans on spore surface occurs when cells are induced to grow in a sporulation medium.

Results

Spores are decorated with two rare sugars, 3-*C*-methyl-6-deoxyhexoses

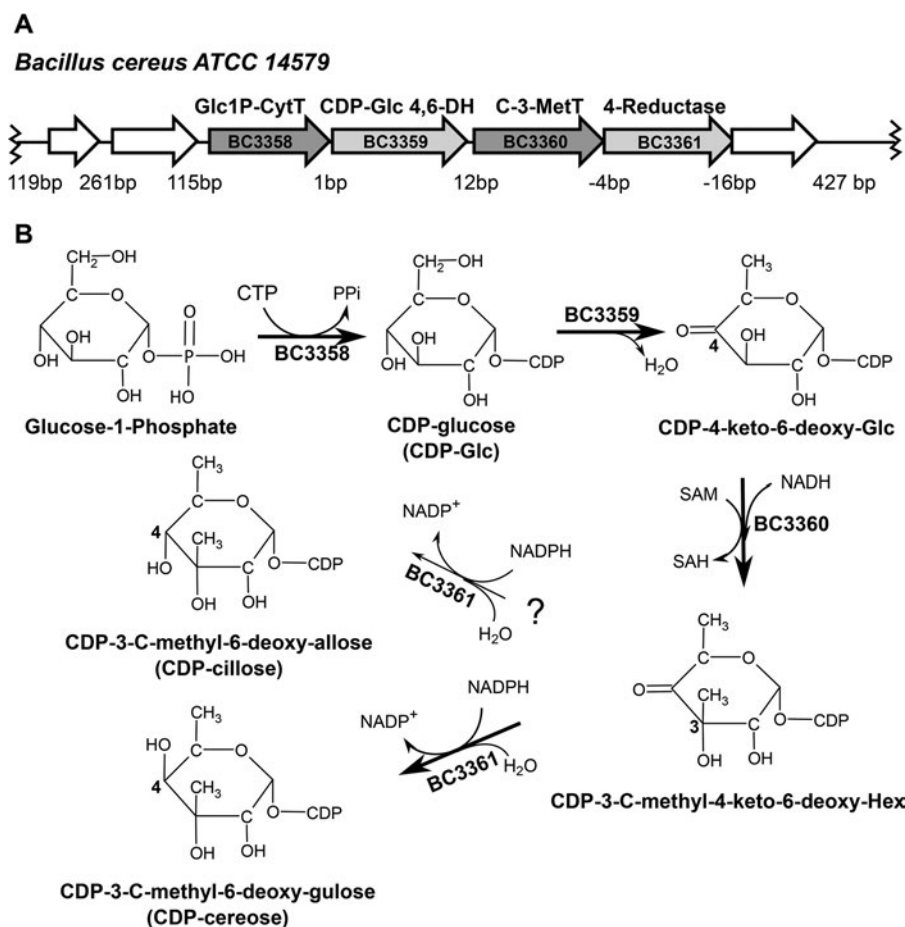
Subtle differences among glycoconjugate structures were proposed to facilitate the specific interaction of a pathogen with its host. Hence, one important task was to determine all sugar residues that decorate a glycan. This becomes difficult when

This work was supported by Grant DE-PS02-06ER64304 from the BioEnergy Science Center, Biological and Environmental Research Program, U.S. Dept. of Energy Office of Science. The authors declare that they have no conflicts of interest with the contents of this article.

The nucleotide sequence(s) reported in this paper has been submitted to the GenBank™/EBI Data Bank with accession number(s) KY445942, KY445943, KY432406, and KY432407

This article contains supplemental Figs. S1–S3 and Tables S1 and S2.

¹ To whom correspondence should be addressed: Complex Carbohydrate Research Center, 315 Riverbend Rd., Athens, GA 30602. Tel.: 706-542-4496; Fax: 706-542-4412; E-mail: peled@ccrc.uga.edu.



different growth environments influence glycan composition. Furthermore, some sugar residues are labile to common harsh hydrolytic conditions (high temperature and high concentration of acid).

In this study, we examined sugar composition under different hydrolytic conditions using *B. cereus* ATCC 14579 cells. In addition, *B. cereus* was grown in different media because its glycans change as the medium is altered (14). Using this approach, we detected two unknown sugar peaks (labeled B and C in Fig. 2A) by GC-MS analysis. The EI-MS² spectra of peaks B and C (Fig. 2A) showed identical fragment ion patterns, suggesting that they are isomers. Calculations of the potential structure of the alditol-acetate derivatives implied that peaks B and C (Fig. 2A) are sugar residues, predicted to be 3-C-methyl-6-deoxyhexoses. The GC chromatograms and MS fragmentation patterns of such structures have not been reported in *Bacillus*. The peaks at *m/z* 245 and 231 (Fig. 2A) suggest a cleav-

age between C3 and C4; the peaks at *m/z* 189, 129, and 87 as well as *m/z* 203 and 143 are likely secondary ion fragments due to the loss of *m/z* 42 (ketene) or 60 (acetate) from *m/z* 231 and 245, respectively. Interestingly, hydrolyses of samples at a very low molarity of trifluoroacetic acid (TFA), HCl, and acetic acid gave different sugar composition profiles. However, no peaks for the B and C sugar residues (Fig. 2A) were observed when samples were hydrolyzed with 2 or 4 M TFA, suggesting that they are labile.

***C3CM* operon harbors a biosynthetic pathway that includes a methyltransferase to form CDP-3-C-methyl-6-deoxyhexoses**

Because sugars B and C (Fig. 2A) were unknown, possibly uncommon, deoxy sugars with a potentially unique 3'-C modification (Fig. 2A), we predicted that their formation would require an enzyme capable of C-methylating its NDP-sugar precursor. We therefore used the amino acid sequence of functional C-3'-methyltransferase from *Micromonospora chalybeata* (15) to BLAST against the translated genome of *B. cereus* ATCC 14579, and this led us to identify a potential gene, BC3360, encoding a protein with 31% amino acid sequence identity. The *M. chalybeata* C-3'-methyltransferase is involved in the formation of dTDP-3-amino-2,3,6-trideoxy-4-

² The abbreviations used are: EI-MS, electron ionization mass spectrometry; HILIC, hydrophilic interaction liquid chromatography; CytT, cytidyltransferase; MetT, methyltransferase; SAM, S-adenosylmethionine; ddw, double-distilled water; IPTG, isopropyl-1-thio-β-D-galactopyranoside; HMBC, heteronuclear multiple bond correlation; DSS, 4,4-dimethyl-4-silapentane-1-sulfonic acid; BHI, brain-heart infusion.

Bacillus operon produces precursor for spore glycosylation

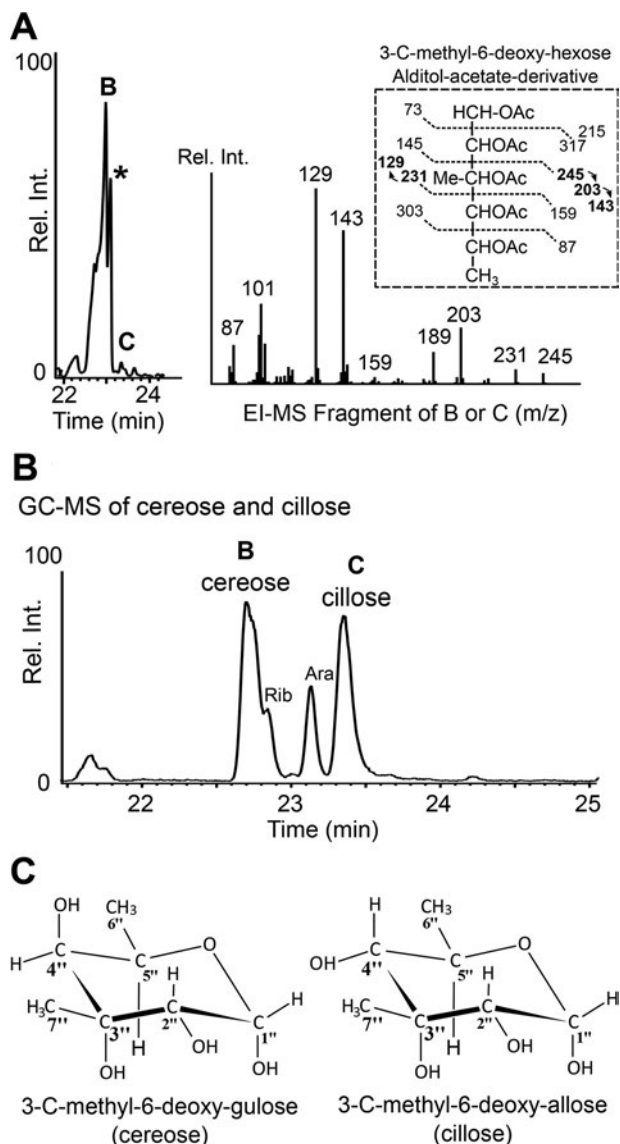


Figure 2. Two uncommon 3-C-methyl-6-deoxyhexose sugar residues were detected upon mild hydrolysis of spore glycans from *Bacillus*. *A*, GC-MS of alditol-acetate derivatives of sugars released by mild acid hydrolyzes from spore glycans of *B. cereus* ATCC 14579 grown in Msgg medium. The two novel sugar peaks eluted at 22.7 and at 23.3 min and are labeled *B* and *C*, respectively. *, 6-deoxyhexose peak. The EI-MS fragmentation pattern of peaks *B* and *C* with their major *m/z* ion fragments is shown in the right spectrum; and the boxed insert shows the predicted primary and secondary MS fragments (labeled in *bold*) of the CDP-3-C-methyl-6-deoxyhexose alditol-acetate derivative. *B*, GC-MS analyses of cereose and cillose standards were obtained from mild hydrolysis of corresponding CDP-3-C-methyl sugars purified from an in-microbe-based assay (see Fig. 4 for CDP-cillose) and after an enzymatic assay (see Fig. 8 for CDP-cereose). Alditol-acetate-sugar derivative peaks of ribose and arabinose are also shown. *C*, structures of cereose and cillose.

keto-3-methyl-D-glucose (dTDP-tetronitrose) (15, 16). This unusual C3-methylated amino-deoxy sugar (tetronitrose) is incorporated from its precursor, dTDP-tetronitrose, to a molecule with antibacterial properties, kijanimicin (17), and to an antitumor agent, tetrocarcin A (16). Although 31% sequence identity is not high (with an expected value of $1e^{-66}$), we were encouraged to pursue this *Bacillus* homologous protein as a candidate methyltransferase (MetT) because it harbors a few

conserved amino acids and domains shared with the *M. chalybeata* C-MetT. Interestingly, flanking the putative *Bacillus* C-methyltransferase are three additional genes predicted to be involved in NDP-sugar synthesis as well (Fig. 1A). However, rather than dTDP-biosynthetic genes as found in *M. chalybeata*, the genes flanking *Bacillus* BC3360 were annotated as CDP-sugar biosynthetic genes.

A proposed biosynthetic pathway of this operon is shown in Fig. 1B. The C3CM operon encodes the following enzymes based on their specific activities (described in detail below): CTP:glucose-1-phosphate cytidylyltransferase (Bc3358, Glc1P-CytT); CDP-glucose 4,6-dehydratase (Bc3359, 4,6-dehydratase); and SAM:CDP-4-keto-6-deoxyglucose C3-methyltransferase (Bc3360, C3-MetT). Subsequently, a CDP-3-C-methyl-4-keto-6-deoxyhexose 4-reductase predominantly forms the final product, CDP-3-C-methyl-6-deoxyglucose.

In-microbe analyses of genes of the C3CM operon in Escherichia coli show synthesis of CDP-3-C-methyl-6-deoxyallose

Of the two experimental approaches used to determine the function of genes within the C3CM operon, the first one is named “in-microbe.” The in-microbe experimental setup consisted of a combination of up to four recombinant genes of the C3CM operon that were co-transformed into *E. coli*. After isopropyl-1-thio- β -D-galactopyranoside (IPTG) gene induction, the NDP-sugars were directly extracted from the cell and separated by HILIC column. Chromatographic peaks were further purified and analyzed by NMR. *E. coli* induced to express the first gene, BC3358, gave a distinct peak (Fig. 3Ai) with an ion $[M-H]^-$ at *m/z* 564 that gave MS/MS ion fragments at *m/z* 322 and 241 (Fig. 3Bi), consistent with CDP-hexose, CMP $[M]^-$, and sugar 1-P $[M-H_2O]^-$, respectively. The *m/z* 564 was not found in control *E. coli* expressing empty plasmid (Fig. 3Av). Subsequently, the *E. coli* (Bc3358)-produced NDP-sugars were purified by HPLC and analyzed by NMR spectroscopy. The NMR data confirmed that the *m/z* 564 peak was CDP-Glc (supplemental Fig. S1). The chemical shift assignments for CDP-Glc are summarized in Table 1. The large $J_{H2'',H3''}$ and $J_{H3'',H4''}$ coupling constants of 9.9 and 9.8 Hz, respectively, are consistent with a sugar in *gluco*-configuration. The chemical shift of 5.59 ppm of the anomeric proton and $J_{H1'',H2''}$ coupling constants of 3.4 Hz are consistent with an α -linkage. This suggests that enzyme Bc3358 is a CTP:glucose-1-phosphate cytidylyltransferase.

E. coli induced to express both BC3358 and BC3359 gave a broad peak eluting from an HILIC column between 16.5 and 18 min. This peak was characterized as CDP-4-keto-6-deoxyglucose (CDP-4k-6d-Glc) (Fig. 3Aii) with an ion $[M-H]^-$ at *m/z* 546 that gave by MS/MS an ion fragment of *m/z* 322 (Fig. 3Bii). This suggests that BC3359 encodes a CDP-glucose 4,6-dehydratase. Similarly, *E. coli* induced to express three *Bacillus* genes (BC3358, BC3359, and BC3360) produced yet another broad peak with a retention time (14–15.5 min) distinct from the previous time shown in Fig. 3Aiii and an ion $[M-H]^-$ at *m/z* of 560 (Fig. 3Biii) that gave MS/MS ion fragments of *m/z* 322 and 237. The empty vector control yielded no *m/z* 560 (Fig. 3Av). This increase of 14 atomic mass units indicates that the

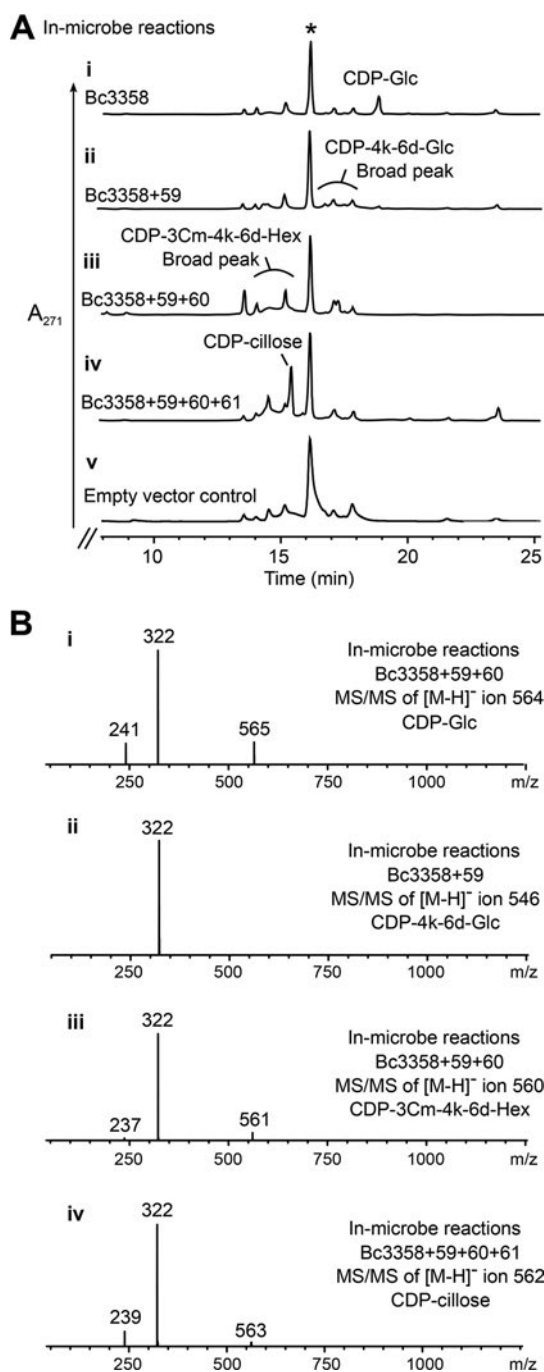


Figure 3. In-microbe analyses of the four genes encoded by the C3CM operon. *A*, HILIC chromatograms of extracts isolated from *E. coli* cells overexpressing combinations of up to four genes: *i*, *E. coli* expressed a single gene, *BC3358*, producing CDP-glucose; *ii*, *E. coli* expressed the combined *BC3358+BC3359* genes, producing CDP-4-keto-6-deoxyglucose; *iii*, *E. coli* expressed the combined *BC3358+BC3359+BC3360* genes, producing a 3-*C*-methylated CDP-4-keto-6-deoxyhexose; *iv*, *E. coli* expressed the combined four genes, producing a new UV peak, later assigned as CDP-cillose; *v*, *E. coli* expressed an empty vector control, producing no such peak. *A₂₇₁* is the maximum absorption for cytosine-based molecule. The large peak (16 min) labeled by an asterisk indicates the internal reference. *B*, LC-MS/MS analyses of each in-microbe reaction product: *i*, CDP-glucose with *m/z* of [M-H]⁻ 564 and its MS/MS fragment products; *ii*, the combined *BC3358+BC3359* produces CDP-4-keto-6-deoxyglucose with *m/z* of [M-H]⁻ 546 and its MS/MS fragment products; *iii*, the combined *BC3358+BC3359+BC3360* genes produce a 3-*C*-methylated CDP-4-keto-6-deoxyhexose glucose with *m/z* of [M-H]⁻ 560 and its MS/MS fragment product; and *iv*, the combined four genes yield CDP-3-*C*-methyl-6-deoxyallose with *m/z* of [M-H]⁻ 562 and its MS/MS fragment product. The control empty vector had no such mass.

Table 1
Chemical shifts for CDP-cillose, CDP-cereose, and CDP-glucose

Nucleotide sugar	H (ppm)	¹³ C (ppm)	<i>J</i> coupling (Hz)
CDP-cillose			
1	5.52	97.70	<i>J</i> _{1,P} = 7.18
2	3.56	73.33	<i>J</i> _{1,2} = 3.79
3		76.28	
4	3.15	77.69	<i>J</i> _{4,5} = 10.10
5	4.08	67.87	<i>J</i> _{5,6} = 5.37
6	1.26	19.46	
7	1.29	23.40	
CDP-cereose			
1	5.54	98.07	<i>J</i> _{1,P} = 7.26
2	3.67	70.67	<i>J</i> _{1,2} = 3.68
3		75.80	
4	3.36	77.89	<i>J</i> _{4,5} < 1
5	4.56	67.10	<i>J</i> _{5,6} = 6.72
6	1.19	18.23	
7	1.31	25.45	
CDP-glucose			
1	5.59		<i>J</i> _{1,P} = 7.1
2	3.52		<i>J</i> _{1,2} = 3.4
3	3.88		<i>J</i> _{2,3} = 9.9
4	3.45		<i>J</i> _{3,4} = 9.8
5	3.76		<i>J</i> _{4,5} = 9.8
6a	3.84		<i>J</i> _{5,6a} = 2.1
			<i>J</i> _{5,6b} = 6.4
6b	3.75		<i>J</i> _{6a,b} = 12.5

three combined *Bacillus* genes yielded a *C*-methylated CDP-4-keto-6-deoxyglucose. The MS/MS of the product (*m/z* 560) gave an ion fragment at *m/z* 237 (Fig. 3*Biii*), consistent with a methyl modification of the 4-keto sugar-1-*P* [M-H₂O]⁻. Hence, we tentatively suggest that *BC3360* encodes a CDP-4-keto-6-deoxyglucose *C3*-methyltransferase. Lastly, when all four genes were co-expressed in *E. coli*, a new peak was observed (Fig. 3*Aiv*) with an ion [M-H]⁻ at *m/z* 562, which gave MS/MS ion fragments of *m/z* 322 and 239 (Fig. 3*Biv*). This increase of 2 atomic mass units indicates that the 4-keto moiety of the substrate is reduced. Such a peak was not detected in the *E. coli* control. Hence, the last gene (*BC3361*) when expressed in *E. coli* suggested encoding a CDP-3-*C*-methyl-4-keto-6-deoxyhexose 4-reductase.

One- and two-dimensional NMR experiments reveal the chemical structure of CDP-3-*C*-methyl-6-deoxyallose

Column purification of the final four-gene product (CDP-3-*C*-methyl-6-deoxyhexose) produced by the in-microbe experiment (Fig. 3*Aiv*, see *peak point* indicated by *arrow*) was analyzed by NMR spectroscopy (Fig. 4*A*). The one-dimensional NMR spectrum (Fig. 4*B*) shows protons H5 and H6 belonging to the Cyt base ring and anomeric signals belonging to ribose H1' (5.98 ppm) and 3-*C*-methyl-6-deoxyallose H1'' (5.52 ppm), as well as ring protons (3–4.5 ppm) and the diagnostic H5'' proton of the 6-deoxysugar. In addition, two distinct signals in the methyl region were observed. The first peak (H7'', 1.29 ppm) is a singlet and was later assigned to the methyl group attached to C3''; the second peak is a doublet and was later assigned to the methyl group at C6''. The singlet peak suggested that no proton is connected to the C3'' on the sugar ring, whereas the doublet peak (*i.e.* split) at H6'' is the result of coupling to H5''. If the C3''-methyl was *O*-linked to C3'' (like in methanol), we would expect a H3'' signal and a doublet signal of H7'' due to the split of H3''.

Bacillus operon produces precursor for spore glycosylation

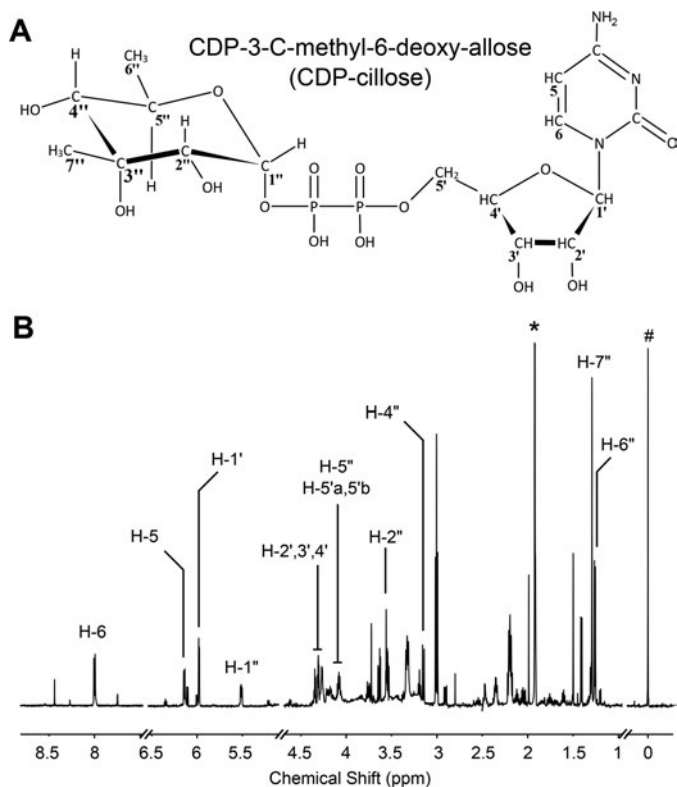


Figure 4. The combined *B. cereus* BC3358+BC3359+BC3360+BC3361 genes expressed in *E. coli* produce CDP-3-C-methyl-6-deoxyallose:CDP-cillose. **A**, structure of CDP-cillose. The specific, numbered protons (*H*) and carbons (*C*) are labeled. **B**, ^1H NMR spectrum of CDP-cillose with selective peak proton signals. The spectrum was cropped to fit the window. * and #, indicate ammonium formate and DSS signals, respectively.

A two-dimensional COSY experiment (Fig. 5A) showed the connectivity between $\text{H}1''$ and $\text{H}2''$, $\text{H}4''$ and $\text{H}5''$, and $\text{H}5''$ and $\text{H}6''$ on the cillose ring. The absence of a proton connected to the $\text{C}3''$ position and the absence of connectivity of methyl $\text{H}7''$ to any adjacent protons suggest that this methyl group is connected via a carbon at the $3''$ position. In addition, our HMBC experiment (Fig. 5B) also indicates the connectivity of methyl $\text{H}6''$ to $\text{C}4''$ and $\text{C}5''$ and methyl $\text{H}7''$ to $\text{C}2''$, $\text{C}3''$, and $\text{C}4''$, suggesting a sugar ring with 3-*C*-methyl-6-deoxyallose configuration.

Complete determination of the stereoisomerism of this nucleotide sugar came by measuring the coupling constants in one-dimensional NMR experiments. The large coupling constant $J_{4,5} = 10.1$ Hz between $\text{H}4''$ and $\text{H}5''$ (Table 1) strongly supports an *allose*-configuration and not a *gulose*-configuration. The distinct chemical shift of the anomeric proton $\text{H}1''$ and the J coupling constant value of 3.79 Hz for $J_{\text{H}1'',\text{H}2''}$ are consistent with α -linkage to the phosphate moiety of CDP. Additionally, a one-dimensional ROESY experiment was performed (Fig. 5C). When $\text{H}4''$ was irradiated, dipolar couplings (NOE effect) between $\text{H}4''$ and $\text{H}2''$, $\text{H}4$ and $\text{H}6''$, and $\text{H}4''$ and $\text{H}7''$ were observed, confirming an *allose*-configuration. Taken together, this nucleotide sugar is characterized as CDP-3-*C*-methyl-6-deoxyallose, which we named CDP-cillose.

In addition to NMR analysis, we also utilized a CDP-cillose sample as a standard for GC-MS analysis. When the CDP-

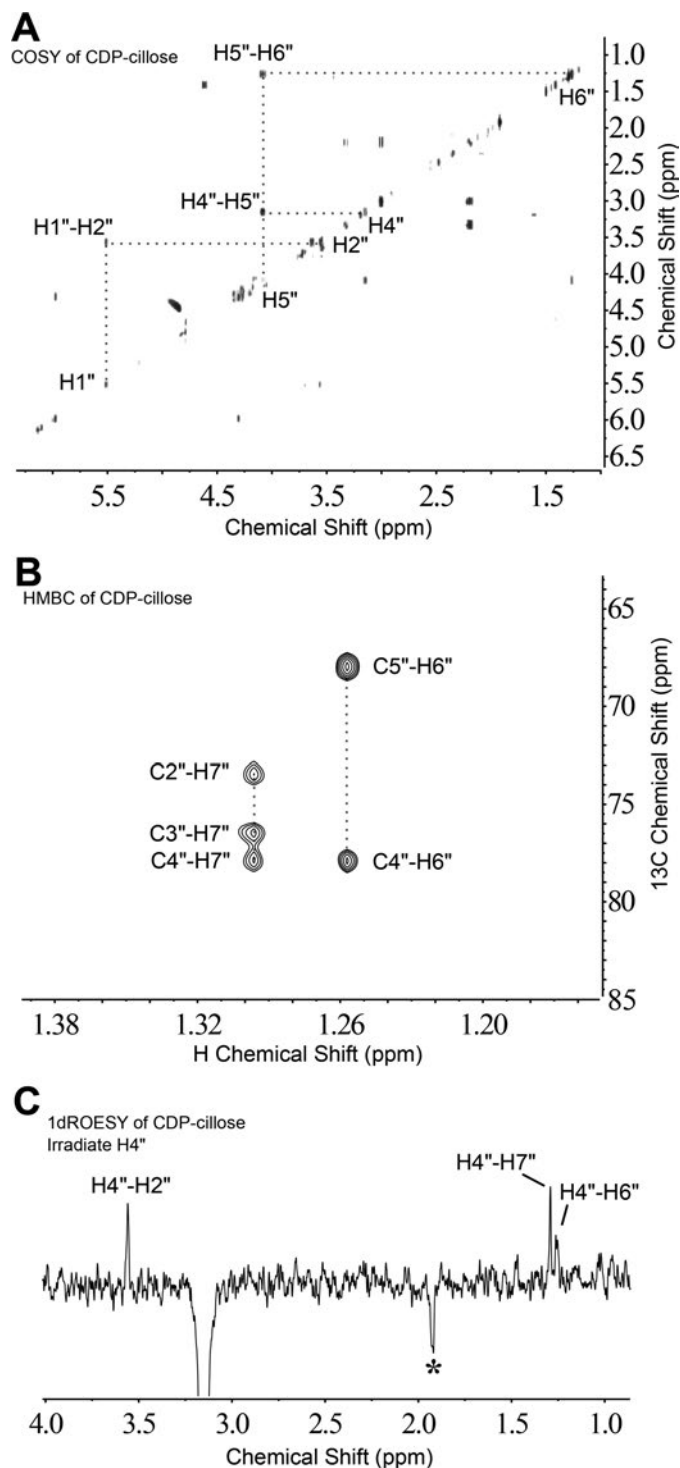


Figure 5. Detailed NMR characterization of CDP-cillose derived by in-microbe HPLC-purified reaction product. **A**, COSY experiment showing the connectivity between protons in the sugar ring moiety that are 2–3 bonds apart. Note that there is no proton connected through $\text{H}2''$ and $\text{H}4''$ indicating no proton linked to $\text{C}3''$. **B**, selected spectral region of HMBC experiment showing protons on the methyl region connected to adjacent carbons that are 2–3 bonds away. Note that the methyl group ($\text{H}7''$) is connected to $\text{C}3''$ indicating that cillose is $\text{C}3$ -methylated. **C**, one-dimensional ROESY experiment with $\text{H}4''$ irradiated. Dipolar couplings (NOE effect) are observed between $\text{H}4''$ and $\text{H}2''$ also indicating an *allose*-configuration.

cillose standard was hydrolyzed, derivatized to its alditol acetate, and analyzed by GC-MS, the retention time, EI-MS ion, and fragments were identical to sugar peak *C* in Fig. 2B.

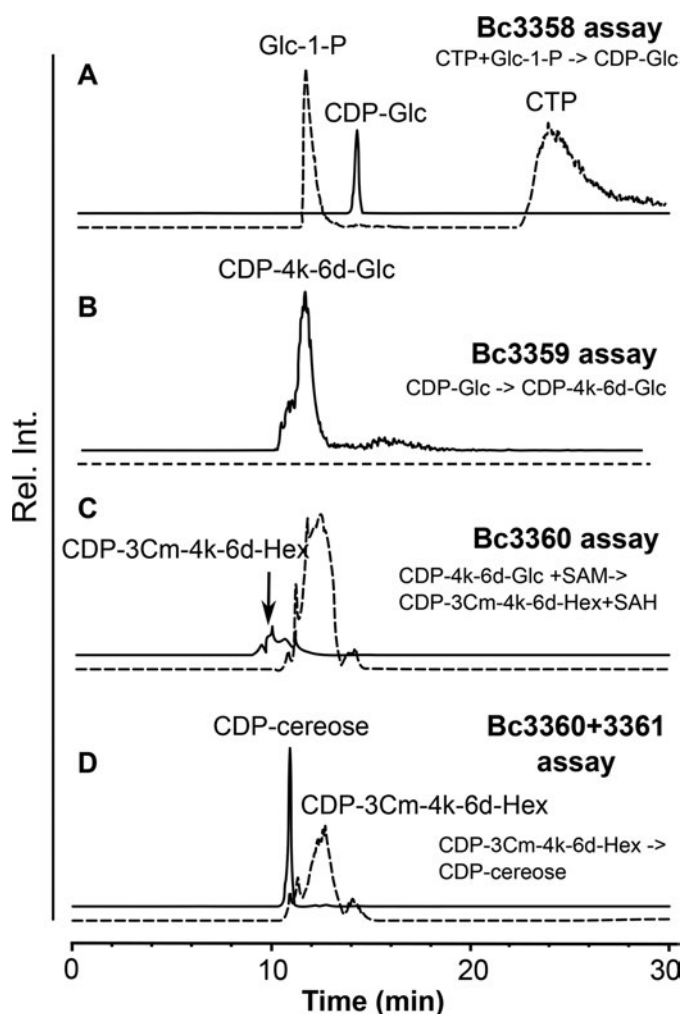


Figure 6. LC-MS *in vitro* enzymatic analyses of purified recombinant proteins encoded by the C3CM operon. *A*, purified His₆-Bc3358 was reacted with CTP and Glc-1-P to yield a new peak of CDP-Glc eluting from HILIC column at 14 min. The *dashed line* indicates the elution of substrates. *B*, purified His₆-Bc3359 converts CDP-Glc to a new peak, CDP-4-keto-6-deoxy-Glc, eluting as a broad peak between 10 and 12 min. *C*, His₆-Bc3360 methylates and converts CDP-4-keto-6-deoxy-Glc to CDP-3-C-methyl-4-keto-6-deoxyhexose. *D*, when reaction shown in *panel B* was terminated and co-incubated with purified His₆-Bc3360 and His₆-Bc3361, a new peak eluting at 11 min was observed; this peak was later identified as CDP-3-C-methyl-6-deoxygulose (CDP-cereose).

***In vitro* assays of C3CM operon reveal that the combined enzymatic product is CDP-3-C-methyl-6-deoxygulose**

Although the first method provided evidence that the four *Bacillus* genes expressed in *E. coli* produced CDP-cillose, the second approach based on *in vitro* enzymatic assays suggests that the last step gives a different product with altered sugar configuration, as described below. In the second method, each individual recombinant protein was expressed and purified by affinity column (supplemental Fig. S2). Our biochemical data confirm that recombinant His₆-Bc3358 is indeed a CTP:Glc-1-P cytidyltransferase as determined by LC-MS/MS (Fig. 6A), whereas the control empty vector gave no product. During the initial characterization of the recombinant enzyme, we determined that the activity required magnesium, Glc-1-P, and CTP, as no activity was observed without the metal. The enzyme is specific to CTP as a nucleotide because ATP, dTDP, and GTP

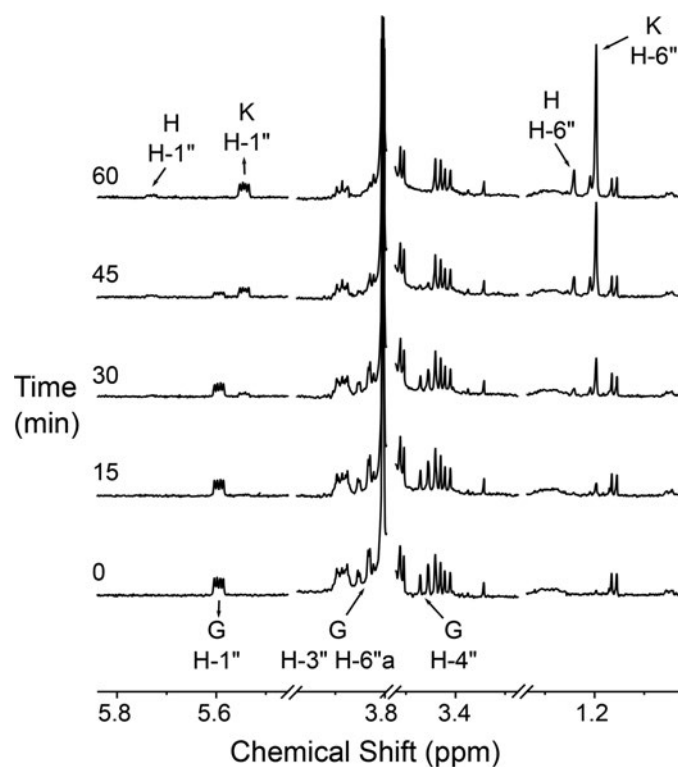


Figure 7. Time-resolved ¹H NMR showing that recombinant Bc3359 is a CDP-Glc 4,6-dehydratase. The enzymatic conversion of CDP-Glc (G) to CDP-4-keto-6-deoxy-Glc (K) and its hydrated form (H) is shown over time by proton NMR. The chemical shift regions of the proton NMR spectrum that are diagnostic for the H-1'' anomeric protons of enzymatic reactant G and products H and K are shown between 5.5 and 5.8 ppm. The diagnostic signals for the three methyl proton (H6'') peaks of products K and H are shown between 1.1 and 1.3 ppm.

are not substrates in the conditions described under “Experimental procedures”; however, a less than 1% conversion was observed with UTP. Gal-1-P is not a substrate. MS analyses of the enzymatic peak product yielded an ion at *m/z* 564 and an MS/MS ion fragment of *m/z* 322, consistent with [CDP-Glc-H]⁻ and [CMP-H]⁻, respectively. As CDP-Glc is unavailable commercially, we purified a large amount of it, using a HILIC column, for further characterization of the subsequent enzymes.

The second enzyme is a specific 4,6-dehydratase. The recombinant enzyme, His₆-Bc3359, readily converted CDP-Glc to a CDP-4-keto-6-deoxygulose, whereas a control reaction yielded no product. Fig. 6B shows LC-MS/MS analyses of the activity of Bc3359, where the enzymatic products (labeled CDP-4k-6d-Glc, referring to CDP-4-keto-6-deoxy-Glc) eluted from the HILIC column as a broad peak between 10 and 12 min and with ion [M-H]⁻ at *m/z* 546. MS/MS analysis of this peak yielded a fragment of 322 *m/z* consistent with CMP. To gain further insight into Bc3359 4,6-dehydratase enzyme activity, we monitored the reaction by time-resolved ¹H NMR. The anomeric signal at 5.59 ppm (Fig. 7 labeled G, H-1''; see 0-min time point) indicates the chemical shift of the substrate, CDP-Glc. As the enzymatic reaction progressed, two new products appeared, each with a quartet of peak signals at 5.56 and 5.74 ppm (Fig. 7 labeled K, H-1'' and H, H-1'') in the anomeric region of the NMR spectrum, whereas the H-1'' of the substrate disap-

Bacillus operon produces precursor for spore glycosylation

peared. Product K is CDP-4-keto-6-deoxy-Glc and H is the hydrated form of K. The H-4'' proton signal of the substrate (labeled C, H-4'') decreased over time, reflecting the disappearance of H-4'' when forming the 4-keto structure product. Two signals also appeared at the 6-deoxy regions around 1.20 and 1.30 ppm. These signals correspond to the C6-methyl protons (H-6'') of products K and H sugar moieties, respectively. The collective MS/MS and NMR data provide evidence that Bc3359 encodes a CDP-Glc 4-6-dehydratase. Further assays were conducted to determine substrate specificity, but dTDP-Glc and UDP-GlcNAc were not substrates; however, less than 1% of the UDP-Glc was converted to UDP-4-keto-6-deoxy-Glc as evident by MS/MS.

The next enzyme activity was found as C3-MetT. Preliminary assays established that the recombinant *Bacillus* Bc3359 C3-MetT requires magnesium and NADH for activity and is SAM-dependent. The purified recombinant C3-MetT (His₆-Bc3360) was reacted with CDP-4-keto-6-deoxyglucose (the reaction product of Bc3359). A new broad peak with a retention time between 9.5 and 10.5 min (Fig. 6C) was detected, whereas a control reaction gave no product. The mass spectrum showed an ion [M-H]⁻ at *m/z* 560, proposing that the product was also a CDP-4-keto-sugar, but the increase of 14 atomic mass units when compared with the substrate suggested that the product gained a methyl group. Hence, the product of Bc3360 is CDP-3-C-methyl-4-keto-6-deoxyhexose. Interestingly, the activity of the C3-MetT was relatively low and only a ~10% conversion was obtained. However, adding the last enzyme in the pathway (4-reductase, Bc3361) drove the reaction further to produce a new product. Fig. 6D shows the enzymatic assay of the combined C3-MetT and 4-reductase. Both purified recombinant C3-MetT (His₆-Bc3360) and 4-reductase (His₆-Bc3361) readily reacted with CDP-4-keto-6-deoxyhexose to yield a final product, whereas negative control reactions gave no product. A peak with a retention time at 11 min (Fig. 6D) was detected having an ion [M-H]⁻ at *m/z* 562. MS/MS analysis of this ion gave fragments at *m/z* 322 and 239, consistent with CMP and sugar-1-P derivatives for CDP-3-C-methyl-6-deoxyhexose.

When substituting Mg²⁺ for Zn²⁺ or Mn²⁺ in the Bc3360 assay, no C3-MetT activity was detected. On omitting NADH, no C3-MetT activity and only low activity was observed when NADPH was substituted for NADH or when pyridoxal phosphate (PLP) was used. Lastly, the C3-MetT activity requires SAM as the methyl donor with the highest activity at 22 °C and with little activity at 37 °C. Further support for the *in vitro* C3-MetT-specific activity came from our in-microbe experiment. Engineered *E. coli* cells co-expressing the C3-MetT gene with a gene encoding an enzyme that forms dTDP-4-keto-6-deoxy-Glc, UDP-4-keto-6-deoxy-Glc, or UDP-4-keto-6-deoxy-*N*-acetylhexosamine were not able to methylate these derivatives. The last enzyme in the pathway is a 4-reductase. It has the highest activity with NADPH rather NADH. In the in-microbe experiments, the 4-reductase activity also appeared specific with no activities toward dTDP-4-keto-6-deoxy-Glc, UDP-4-keto-6-deoxy-Glc, or UDP-4-keto-6-deoxy-*N*-acetylhexosamine.

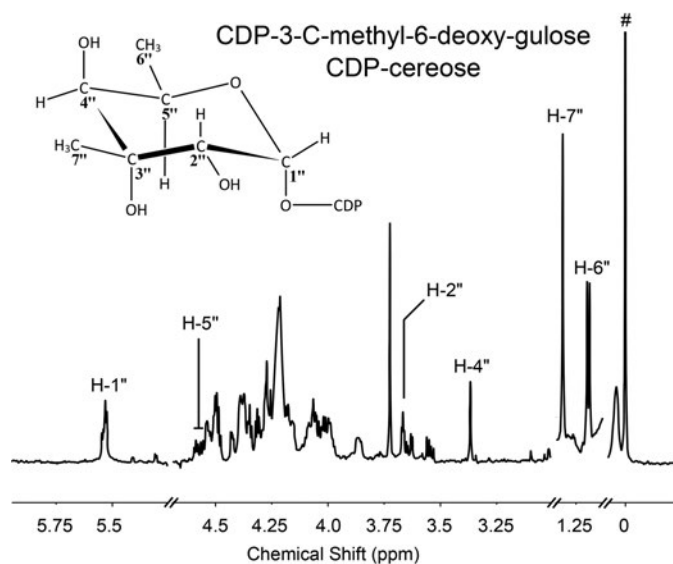


Figure 8. One-dimensional proton NMR spectrum of the combined four-gene *in vitro* enzymatic product shows that the product is CDP-3-C-methyl-6-deoxygulose:CDP-cereose. Selected signals are labeled on the spectrum. #, indicates DSS signal.

One- and two-dimensional NMR reveals the chemical structure of CDP-3-C-methyl-6-deoxygulose

The column-purified product (see product peak in Fig. 6D) of the *in vitro* combined enzymatic assays of His₆-Bc3360 and His₆-Bc3361 was analyzed by NMR spectroscopy. The one-dimensional NMR spectra (Fig. 8) showed anomeric signals belonging to the H1'' peak (5.54 ppm), ring protons H2'' and H4'' (3.25–3.75 ppm), and the diagnostic H5'' proton of the 6-deoxy-sugar (4.56 ppm). Similar to CDP-cillose, two distinct methyl signals were observed: the singlet peak H7'' (1.31 ppm), which represents the methyl group attached to C3''; and the doublet peak H6'' (1.19 ppm), assigned to the methyl group at C6''. The chemical shifts acquired are different from those of CDP-cillose, indicating that the enzymatic product from the *in vitro* assay of the C3CM operon is different from the *E. coli*-based in-microbe reaction. The chemical shift differences between CDP-cillose made in *E. coli* compared with the *in vitro* enzymatic product led us to acquire more NMR data to determine the structural nature of this material.

Further two-dimensional COSY and ROESY experiments were performed to determine the stereoisomerism of H4'' (Fig. 9). The COSY experiment (Fig. 9A) showed the connectivity between H1'' and H2'' and H5'' and H6'' on the ring. No proton connected the C3'' position, as expected; however no coupling between H4'' and H5'' was observed, indicating that the coupling constant between H4'' and H5'' is very small ($J_{4,5} < 1$). An additional ROESY experiment was conducted to confirm that H4'' is in an axial position (Fig. 9B). Dipolar couplings were observed between H4'' and H6'' and H4'' and H7'', but no NOE effect was observed between H4'' and H2'' (data not shown), suggesting that H4'' is in an axial position, consistent with a *gulose*-configuration. The NOE effect observed between H2'' and H7'' (Fig. 9B) also indicates that the methyl on C3'' is equatorial. Taken together, the product of the *in vitro* enzymatic assay from the C3CM operon is CDP-3-C-methyl-6-deoxygu-

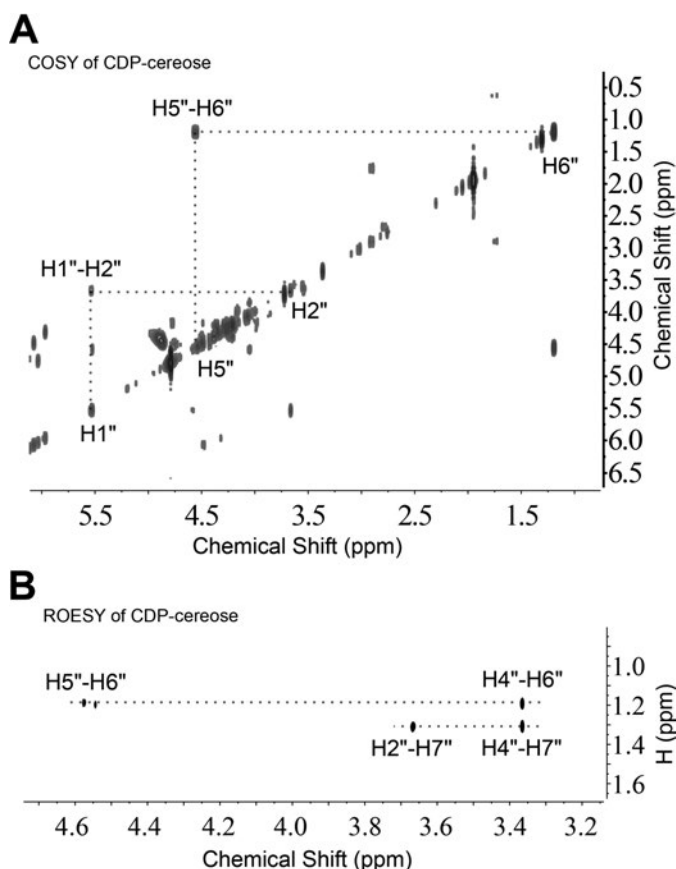


Figure 9. Detailed NMR characterization of CDP-cereose derived by *in vitro* assays. A, COSY experiment showing the connectivity between protons in the sugar ring moiety that are 2–3 bonds apart. Note that there is no proton connected to H2', and the *J* coupling between H4' and H5' is too small to observe, indicating that H4' is in an axial position. B, selected spectral region of ROESY experiment showing dipolar couplings (NOE effect) between H4' and H6', H4' and H7', H5' and H6', and H2' and H7', indicating a *gulose*-configuration.

lose. We decided to name it CDP-cereose because while this work was in progress, a study on spore glycoprotein BclA in *B. cereus* ATCC 14579 (18) identified cereose as attached as a terminal sugar that is β -1,4-linked to 3-*O*-methyl-rhamnose on the oligosaccharide of BclA. The complete chemical shifts of CDP-cereose are listed in Table 1. We also utilize a purified CDP-cereose sample as a standard for the GC-MS analysis, and the retention time, the EI-MS ion, and fragments are identical to sugar peak B in Fig. 2B.

To solve the discrepancy between the *E. coli* *in*-microbe analysis and the *in vitro* enzymatic activities, we decided to examine whether the 4-reductase is also a 4-epimerase. However, CDP-cillose was not converted by Bc3361 to CDP-cereose when assays utilized NADPH or NADH as determined by NMR.

***Bacillus* produces predominantly CDP-cereose *in vivo* during sporulation**

We next addressed which CDP-3-*C*-methyl-6-deoxyhexose sugar(s) *Bacillus* produces *in vivo* and when. For that purpose we analyzed NDP-sugars as well as the expression of genes belonging to the C3CM operon. We first examined whether the genes are constitutively expressed or are induced by specific environmental cues. To that end we found that rich BHI (brain-

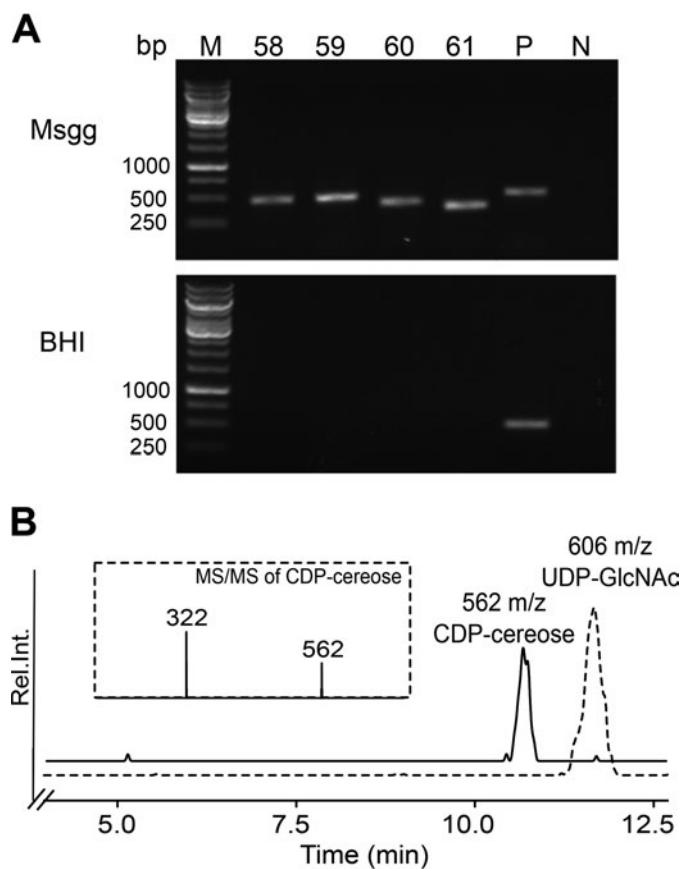


Figure 10. *Bacillus* produces predominantly CDP-cereose *in vivo* during sporulation. A, genes of the C3CM operon are transcribed during growth in Msgg liquid medium but are not transcribed in rich BHI medium, which maintains vegetative growth. RT-PCR analysis for the expression of gene encoding: lane 58, BC3358; lane 59, BC3359; lane 60, BC3360; lane 61, BC3361; lane P, sigA positive control; lane N, negative control (RT-PCR reaction without RT). B, LC-MS/MS analysis of nucleotide-sugar extracts from *B. cereus* ATCC 14579 grown in Msgg medium for 2 days. The data were selected to show only [M-H]⁻ ions at *m/z* 562 for CDP-3-*C*-methyl-6-deoxyhexose and *m/z* 606 for UDP-GlcNAc as a reference. The MS/MS fragmentation pattern of ion 562 *m/z* is shown in the dotted-line box.

heart infusion) medium suppressed transcription of the four genes (Fig. 10A), whereas under a defined nutrient medium (Msgg) these genes were transcribed as determined by RT-PCR. It took, however, about 48 h for the genes of the C3CM operon to be transcribed upon shifting from BHI to Msgg medium.

Because Msgg medium gave rise to both biofilm and spores, we tested whether DSM (Difco sporulation medium), which induces spore formation, also gave rise to an accumulation of CDP-3-*C*-methyl-6-deoxyhexose. To that end, NDP-sugars were extracted from *Bacillus* grown in either Msgg or DSM. A peak with a retention time at 11 min (Fig. 10B) was detected with *m/z* 562, an ion consistent with CDP-3-*C*-methyl-6-deoxyhexose. In both DSM and Msgg the *m/z* 562 was identified on the first day, with the highest level at day 2 and reduced amounts by day 4. The HILIC column was unable to separate the CDP-cillose from its 4-epimer, CDP-cereose. To determine the identity of peak 562, the NDP-sugars were isolated, mildly hydrolyzed, derivatized to alditol acetates, and analyzed by GC-MS. The elution time (22.7 min) and MS fragmentation data indicate that the major CDP-sugar is CDP-cereose (data not shown). Based on the retention time (23.3 min), the amount

Bacillus operon produces precursor for spore glycosylation

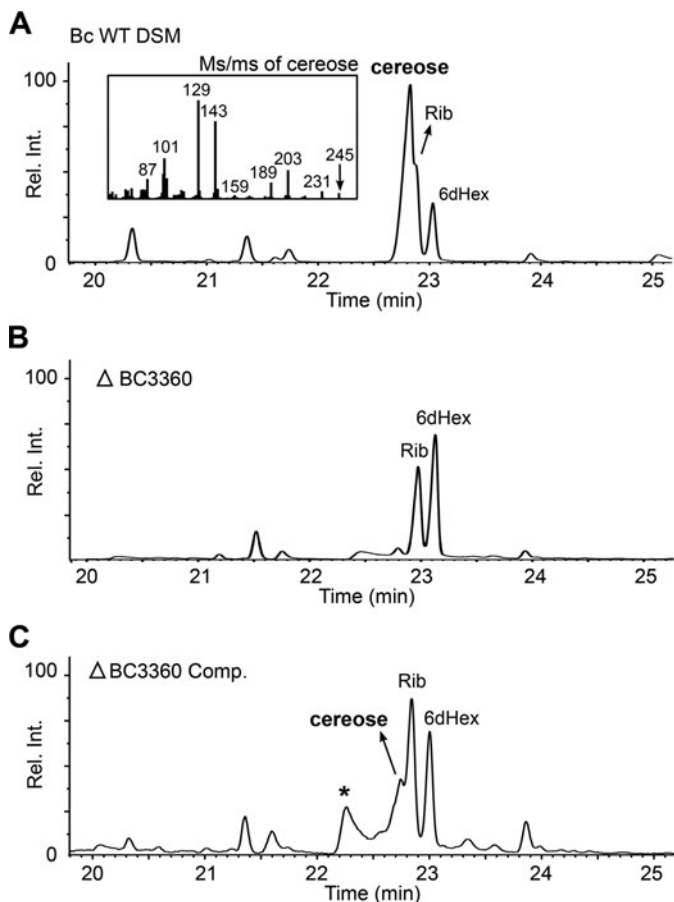


Figure 11. GC-MS of alditol-acetate derivatives of sugars released by mild acid hydrolyzes from spores of wild-type *B. cereus* ATCC 14579 (A), Δ BC3360 (B), and Δ BC3360 (C) complementation strains. All strains were grown on DSM sporulation agar plates. *, unknown contaminant (non-sugar peak).

of cillose derived from CDP-cillose was too low to be designated conclusively. Hence, the combined LC-MS and GC-MS data suggest that *Bacillus* makes predominately CDP-cereose *in vivo*, but we cannot exclude the possibility that CDP-cillose is made, albeit in substantially smaller amounts.

C3CM operon is required to form cereose-containing glycan

We first addressed whether the C3CM operon is involved in cereose-glycan formation. For this purpose, we deleted the gene encoding Bc3360, the C3-MetT in *B. cereus* ATCC 14579 (supplemental Fig. S3). The data of spore-derived glycans in Δ BC3360 not surprisingly showed the lack of the cereose sugar residue (Fig. 11). These data suggested that genetically C3-MetT of the C3CM operon is involved in cereose-containing spore glycans. We then examined genetically the function of Bc3361 and whether it is a specific 4-reductase. To that end, we generated a *BC3361* gene deletion strain, Δ BC3361. The spore glycans were analyzed by GC-MS, and the data showed a significant reduction in the amount of cereose. This strongly suggests that Bc3361 is indeed involved in the formation of cereose-containing glycans in spores. Further investigation and protein crystallography will be required to fully understand the contribution of Bc3361 to the formation of cillose-containing glycans.

We next addressed whether all *Bacillus* sp have the capability of forming cereose-containing glycans. We examined 17 differ-

Table 2

Different strains in *Bacillus* correlate with C3CM operon and cereose production in spores

<i>Bacillus</i> strain	C3CM operon in genome	Cereose production in spores
<i>B. thuringiensis israelensis</i> ATCC 35646	No	No
<i>B. thuringiensis berliner</i> ATCC 10792	Yes	Yes
<i>B. thuringiensis kurstaki</i> HD73	Yes	Yes
<i>B. cereus</i> ATCC 14579	Yes	Yes
<i>B. cereus</i> ATCC 10876	Yes	Yes
<i>B. anthracis</i> 34F2	No	No
<i>B. subtilis</i> PY79	No	No
<i>B. megaterium</i> QMB1551	No	No
<i>B. thuringiensis</i> FSL W8-0767	Yes	Yes
<i>B. thuringiensis</i> FSL W8-0640	Yes	Yes
<i>B. thuringiensis</i> FSL K6-0043	Yes	Yes
<i>B. thuringiensis</i> FSL K6-0073	Yes	Yes
<i>B. thuringiensis</i> FSL W8-0824	Yes	Yes
<i>B. thuringiensis</i> FSL W8-0050	Yes	Yes
<i>B. thuringiensis</i> FSL W8-0275	Yes	Yes
<i>B. wiedmannii</i> FSL K6-0069	Yes	Yes
<i>B. cereus</i> FRI-35	Yes	Yes
<i>B. megaterium</i> QMB1551	No	No

ent *Bacillus* strains (Table 2) of the *Bacillus cereus sensu lato* group: *B. cereus*, *Bacillus thuringiensis*, and *B. anthracis*. Genomic sequences revealed that four of the 17 strains do not harbor DNA sequences for the C3CM operon; and these strains showed no cereose residue by GC-MS. But all strains having the C3CM operon produced cereose. Thus, it is evident that the C3CM operon is indeed involved in the formation of cereose-containing glycans.

C3CM operon may contribute to spore germination

We next addressed whether mutants of the C3CM operon have an effect on spore properties, sporulation, or spore germination. Upon the initial analysis of Δ BC3360 and Δ BC3361, we did not detect any difference in the sporulation rate after 8 days of growth on DSM-agar plates compared with the wild type. Similarly, the lack of 3C-methyl sugars had no impact on spore stability, and mutant spores preincubated at 80, 85, and 90 °C had similar heat stability properties as the wild type (data not shown). However, we observed a 10–20% increase in the germination rate of Δ BC3360 and Δ BC3361 when compared with the wild type (Fig. 12). Taken together, cereose glycosylation may contribute to spore germination but seems not to impact the stability of spores under heat.

Timing of cereose-containing glycan expression

In Mmsg or DSM, over 90% of the *B. cereus* ATCC 14579 cells sporulated by day 3–4. Analyses of glycans isolated from 1-day cultures provided no evidence of cereose-containing glycans. Cereose-containing glycans started to appear in day 2–3 in cultures, with higher amounts accumulating by day 6. To determine whether cereose-containing glycans are stable, we analyzed spores isolated from cultures grown for up to 14 days in Mmsg. No degradation of the cereose-sugar signal was observed between days 6 and 14, suggesting that cereose-containing glycans were not degraded. Similar amounts of cereose were observed in spores produced by DSM. In general, the amount of cillose-containing glycans, based on GC-MS analyses, was not sufficient to be quantified for the timing analysis when compared with cereose-containing glycans.

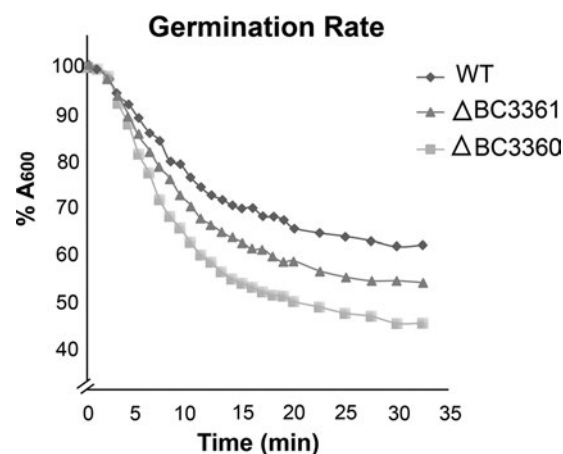


Figure 12. Mutants $\Delta BC3360$ and $\Delta BC3361$ germinate faster than parental wild-type *B. cereus* ATCC 14579. Germination of spores was determined by the relative decrease in spore optical density at $A_{600\text{ nm}}$ over time. The data represent the average of two separate experiments.

The amount of cereose in spores was calculated to be 0.2–1% of the dry mass. This significant amount may play an important role in spore biology.

Cereose sugar is not exclusive to spore glycoprotein BclA

Following the identification of CDP-cereose in this report, we further examined whether cereose is found only in BclA and enriched in the spores by analyzing the enriched exosporium fraction in the BclA mutant as described earlier (18, 19). Cereose indeed appeared in the exosporium preparation, but a significant amount of cereose was also detected in the spores lacking exosporium (Fig. 13A), suggesting that cereose may not be unique to BclA glycoprotein. In addition, upon examination of the BclA as well as the ExsJ mutants from *B. cereus* ATCC 10876 (20), we found cereose present in the spores indicating that cereose may be attached to other glycans as well (Fig. 13B).

Consistent with the above observation, we treated the spores with urea and SDS, as the combined reagents are known to release glycoproteins such as BclA (21) and BclB (22). Analysis of *B. cereus* ATCC 14579 spores after urea/SDS treatment showed two clear GC-MS signals for cereose and cilliose at a ratio of 36:1, respectively (Fig. 13C). This suggests that a large portion of the cereose- and cilliose-containing glycans still decorates the spores. The explanation for this will require further intensive research; it could suggest that some of the cereose/cilliose glycan structures on the spores are either cross-linked to other macromolecules, urea-resistant glycoproteins, or SDS-resistant glycolipids.

Discussion

In this study, we have identified and biochemically characterized a new metabolic pathway involved in the formation of uncommon sugar residues in *Bacillus*. The characterized pathway includes four *B. cereus* ATCC 14579 recombinant proteins (Bc3358–Bc3361). Fig. 1 summarizes our proposed biochemical route for the formation and conversion of CDP-glucose to CDP-3-C-methyl-6-deoxyglucose (named CDP-cereose) and potentially its 4-epimer CDP-cilliose. The first Bc3358 protein is a magnesium- and CTP-dependent enzyme that attaches the

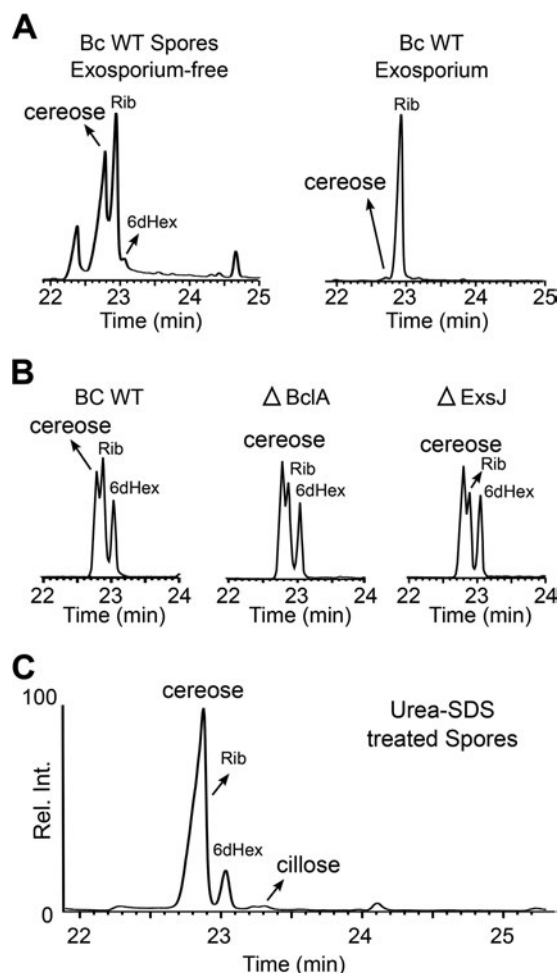


Figure 13. Cereose-containing glycans are not exclusive to the major spore glycoprotein, BclA. Shown are results of GC-MS of alditol-acetate derivatives of sugars released by mild acid hydrolysis from: exosporium-free spore of *B. cereus* ATCC 14579 and exosporium fraction (A); spores of wild-type *B. cereus* ATCC 10876 and glycoprotein mutants $\Delta BclA$ and $\Delta ExsJ$ (20) (B); and urea-SDS-treated spores of wild-type *B. cereus* ATCC 14579 (C).

cytidyl group from CTP to Glc-1-P to from CDP-glucose. The second enzyme, Bc3359, is a specific 4,6-dehydratase that converts CDP-Glc to a CDP-4-keto-6-deoxy-Glc. This intermediate exists in two forms, the hydrated and keto forms. Existing in two forms appears to be a common feature observed with other 4-keto nucleotide-sugar derivatives including UDP-4-keto-6-deoxyglucose (23), UDP-4-keto-6-deoxy-AltNac (24), UDP-4-keto-6-deoxy-GlcNac (25), and UDP-4-keto-xylose (26). The third enzyme is a distinct C3-methyltransferase (C3-MeT, Bc3360) that requires magnesium to catalyze the transfer of the methyl group from SAM and link it to C3' of the sugar moiety of the CDP-sugar to form CDP-3-C-methyl-4-keto-6-deoxyhexose. Like some other characterized C3-methyltransferases (27, 28), Bc3360 is NADH-dependent. There is no apparent formation of NAD^+ , and the enzyme does not appear to function as a reductase in the absence of SAM. It is also able to use NADPH as co-factor with 50% less conversion than NADH as a co-factor. Other co-factors, like pyridoxal phosphate (PLP), which may be suitable for other C3-methyltransferase (29), showed very little conversion (less than 1%). Finally, *in vitro* Bc3361 reduces in an NADPH-dependent manner the 4-keto

Bacillus operon produces precursor for spore glycosylation

moiety of the methyl sugar and converts it to CDP-cereose and NADP. The analog, NADH, could not substitute for NADPH in the 4-reductase reaction.

The order of genes within the C3CM operon, the nucleotide space, and the overlap among the genes are highly similar to other *Bacillus* spp. For example, *BC3360* is overlapped by one nucleotide with *BC3361* and 1- and 12-nucleotide gaps are found between the coding regions of *BC3358* and *BC3359* and *BC3359* and *BC3360*, respectively. Such gene overlaps and reading-frame offsets appeared to be conserved in other *Bacillus* spp including *Bacillus weihenstephanensis* FSL R5-860, *B. cereus* ATCC 10876, *B. thuringiensis* serovar israelensis ATCC 35646, *B. thuringiensis* serovar kurstaki str. HD-1, *Bacillus toyonensis* BCT-7112, and *B. cereus* m1293. It is therefore possible that the expression of the C3CM genes is under the same regulation mechanism. Not all strains of the *B. cereus* group harbor the C3CM operon; for example the *B. anthracis* strains including 34F2, Ames, and Vollum do not have the C3CM genes in their genome. On the other hand, some *B. cereus* strains that are also human pathogens (supplemental Table S1), like *B. cereus* G4264 and G9241 or food and dairy spoilage strains like *B. wiedmannii*, do have C3CM operon. This suggests that cereose decoration on spores may function in assisting spore survival under certain environmental conditions or in host infection via specific mechanisms.

The enzyme activity of recombinant proteins showed that the last protein, a 4-reductase, gave a gulose-configured sugar residue, cereose. However, in *E. coli* the 4-reductase produces predominantly the 4-epimer with an *allose*-configuration, cillose. The discrepancy was not easily discerned, specifically because cillose and cereose are both present in *Bacillus*. One possibility is that the predominant activity of the 4-reductase is to generate CDP-cereose, and little activity is expended to form CDP-cillose. The second possibility is that an additional 4-epimerase in *Bacillus* or *E. coli* epimerizes CDP-cereose to CDP-cillose; or alternatively, the 4-reductase activity could be regulated post-translationally by other factors, resulting in this enzyme having a different activity compared with its activity *in vitro*. The specific mechanism behind this variance is unknown. Further protein crystallography will be required to elucidate the enzymology of Bc3361.

Experimental procedures

Strains and culture conditions

The strains used in this study are listed in Table 2. Each strain was stored in 16% glycerol at -80°C . The media (agar or liquid) used were Luria Bertani (LB) (10 g/liter tryptone, 5 g/liter yeast extract, and 10 g/liter NaCl), BHI, DSM, and Msgg medium (30). *E. coli* DH10B cells were used for cloning and Rosetta2(DE3)pLysS (Novagen) cells were used to express protein.

B. cereus cells were cultured in either liquid or agar plates with Msgg or DSM plates and incubated at 30°C for 5 days to achieve a sporulation rate over 90% as confirmed by microscopy and cfu counts after an 80°C heat stability treatment. The spores were purified as described (31), subsequently washed

repeatedly with sterile double-distilled water (ddw), and finally centrifuged ($8000 \times g$, 10 min).

Cloning the C3CM operon genes

A single colony of *B. cereus* cells grown on BHI-agar was suspended in $50\ \mu\text{l}$ of sterile ddw, heated for 5 min at 95°C , and then centrifuged ($10,000 \times g$, 30 s). A portion of the supernatant ($5\ \mu\text{l}$) was used as the DNA source to amplify each specific gene by PCR. Each primer was designed to include a 15-nucleotide extension with exact sequence homology to the cloning site of the target plasmid at the 5'-end. This facilitated cloning between the NcoI and Bpu1101I sites of pET28_Tev1.15 (32) or the SacI site of the pCDF-ParaB vector. pCDF-ParaB is a modified pCDF duet where expression is controlled by arabinose via the regulator gene *araC*. The pET28_Tev1.15 vector was (32) opened with primer sets ZL169 and KB_T7t. The individual genes (*BC3358*, *BC3359*, *BC3360*, and *BC3361*) were PCR-amplified with primer sets KB2 S and KB2 AS; KB5 S and KB5 AS; KB3 S and KB3 AS; and KB4 S and KB4 AS, respectively (see supplemental Table S2), using high fidelity *Pyrococcus* DNA polymerase (0.4 unit of Phusion Hot Start II, Thermo Scientific), including buffer, dNTPs ($0.4\ \mu\text{l}$ at 10 mM), *B. cereus* DNA template ($5\ \mu\text{l}$), and PCR primer sets ($1\ \mu\text{l}$ each at $10\ \mu\text{M}$) in a $20\text{-}\mu\text{l}$ reaction volume. The PCR conditions were: a 98°C denaturation cycle for 30 s followed by 25 cycles (8 s denaturation at 98°C , 25 s annealing at 54°C , and 20 s elongation at 72°C) and 4°C . After PCR, portions ($2\ \mu\text{l}$ each) of the amplified vector and insert were mixed, treated for 15 min at 37°C with 0.5 unit of FastDigest DpnI (Thermo Scientific), and then transformed into DH10B (Life Technologies)-competent cells. Positively transformed clones were selected on LB-agar containing kanamycin ($50\ \mu\text{g}/\text{ml}$ for pET vector) or spectinomycin ($100\ \mu\text{g}/\text{ml}$ for pCDF vector). Clones were verified by PCR and DNA sequencing. The resulting recombinant plasmids are: pET28b:His₆-Tev-Bc3358#3 yielding N-terminal His₆-Tev-tagged Glc1P-CytT; pET28b:His₆-Tev-Bc3359#10 yielding N-terminal His₆-Tev-tagged CDP-Glc 4,6-DH; pET28b:His₆-Tev-Bc3360#12 yielding N-terminal His₆-Tev-tagged C3-MetT; and pET28b:His₆-Tev-Bc3361#2 yielding N-terminal His₆-Tev-tagged 4-reductase. Plasmids were isolated and purified using a PureLink Quick Plasmid miniprep kit (Invitrogen) and transformed into Rosetta2(DE3)pLysS-competent cells for recombinant protein expression. Once protein activities were confirmed, the DNA sequences of the plasmids harboring specific genes were deposited in GenBank™ with the following accession numbers: KY445942 for Bc3358, KY445943 for Bc3359, KY432406 for Bc3360, and KY432407 for Bc3361.

For C3CM operon gene stacking, plasmid pET28_Tev harboring *BC3359* was used as a secondary vector for the insertion of Bc3360. Vector pET28b:His₆-Tev-Bc3359 and insert pET28b:His₆-Tev-Bc3360 were amplified with primer sets ZL190 and ZL191 and ZL192 and ZL193, respectively (see supplemental Table S2) and cloned as stated previously. The resulting construct, pET28b:His₆-Tev-Bc3359+His₆-Tev-Bc3360, was then used as a tertiary vector for the insertion of *BC3358*. Vector pET28b:His₆-Tev-Bc3359+His₆-Tev-Bc3360 and insert pET28b:His₆-Tev-Bc3358 were amplified with primer sets ZL194 and ZL195 and ZL196 and ZL197, respectively, and

cloned as stated previously. The resulting construct, pET28b: His₆-Tev-Bc3358+His₆-Tev-Bc3359+His₆-Tev-Bc3360, was verified by PCR and DNA sequencing, co-transformed with pCDF-Parab:Bc3361-His₆ plasmid, and cloned by primer sets JGI001 and JGI002 into Rosetta2(DE3)pLysS-competent cells for C3CM recombinant proteins co-expression.

His₆-tagged protein expression and purification

Rosetta2(DE3)pLysS strains harboring pET expression plasmids were grown at 37 °C and 250 rpm in 250 ml of LB medium supplemented with chloramphenicol (35 µg/ml) and kanamycin (50 µg/ml). Gene expression was induced when cellular A₆₀₀ reached 0.6 by adding 0.5 mM IPTG. After induction, cells were grown for 18 h at 18 °C and 250 rpm and then harvested by centrifugation (6000 × g) for 10 min at 4 °C. The cell pellets were washed with ddw and then suspended in 10 ml of lysis buffer (50 mM Tris-HCl, pH 7.4, 10% (v/v) glycerol, 1 mM EDTA, 2 mM DTT, and 0.5 mM PMSF). Cells were lysed by sonication (26), and after centrifugation (6000 × g for 15 min at 4 °C), the supernatant was supplemented with 1 mM DTT and 0.5 mM PMSF and again centrifuged (20,000 × g for 30 min at 4 °C). The supernatant was applied to a nickel-Sepharose fast-flow column (GE Healthcare Life Sciences; 2 ml of resin packed in a polypropylene column, inner diameter 1 × 15 cm). Each column was pre-equilibrated with buffer A (50 mM Tris-HCl, pH 8, 4% (v/v) glycerol, and 100 mM NaCl). The column was washed with 30 ml of buffer A containing 20 mM imidazole and then with 10 ml of buffer A containing 40 mM imidazole. His-tagged proteins were eluted with 5 ml of buffer A containing 250 mM imidazole. The eluates containing these proteins were divided into small aliquots, flash-frozen in liquid nitrogen, and kept at -80 °C. Proteins were separated by SDS-12.5% PAGE and visualized by staining with Coomassie Blue.

Nucleotide-sugar analyses derived from "in-microbe"-based assay

Nucleotide sugars produced by the C3CM operon were extracted as described previously (33). Briefly, Rosetta2(DE3)pLysS strains harboring expression plasmids were grown at 37 °C and 250 rpm in 5 ml of LB medium supplemented with chloramphenicol (35 µg/ml) and kanamycin (50 µg/ml) (pET vector) or with chloramphenicol (25 µg/ml) and kanamycin (35 µg/ml) with additional spectinomycin (35 µg/ml) (pET plus pCDF vector co-expression). Gene expression was induced after 2 h by adding 0.5 mM IPTG. After induction, cells were grown for 3–4 h at 30 °C and 250 rpm and then harvested by centrifugation (10,000 × g, for 1 min at 2 °C). The cell pellets were washed with 4 volumes of 10 mM sodium phosphate, pH 7.5, and 150 mM NaCl (PBS) and then suspended in 1 volume of ddw. Ten volumes of cold chloroform/methanol (1:1, v/v) was added, and the sample was mixed for 15 min on ice. Samples were centrifuged (12,000 rpm, 3 min, 22 °C), and the upper aqueous phase enriched in nucleotide sugar was collected. Portions of this aqueous phase were chromatographed on an HILIC column with HPLC-UV or LC-ESI-MS/MS (liquid chromatography-electrospray ionization-tandem mass spectrometry), using a Shimadzu ESI-MS/MS IT-TOF mass spectrometry system that included a Nexera UFPLC LC-30AD pump, a Sil-

30AC autosampler, and a column heater at 37 °C. HPLC peaks of nucleotide sugars were detected by UV A_{271 nm} (maximum for CDP-sugars), collected, and lyophilized prior to analysis by NMR. The purified product of His₆Bc3358 (CDP-Glc) was also used as substrate for the downstream enzymatic reactions. The purified product of entire C3CM operon (CDP-cillose or CDP-cereose) was suspended in D₂O (99.9%) for NMR analysis.

For analyses by HPLC-UV or LC-MS/MS, an Accucore 150 Amide HILIC column (150 × 4.6 mm, 2.6-µm particle size, Thermo Scientific) was used for chromatography with a solvent system of 40 mM ammonium acetate, pH 4.3 (solvent A), and acetonitrile (solvent B). The column was equilibrated at 0.4 ml/min with 25% A and 75% B prior to sample injection (20 µl). Following injection, the HPLC conditions were: 0–1 min, 0.4 ml/min with 25% A/75%B and then a gradient to 50% A and 50% B over 24 min. The flow rate was then increased to 0.6 ml/min with a gradient to 25% A and 75% B over 5 min. The column was then washed for 5 min with 25% A/75% B prior to the next injection.

In vitro enzyme reactions

The activity of recombinant His₆Bc3358 (referred to herein as Bc3358 or Glc1P-CytT) was examined by HPLC-UV and LC-ESI-MS/MS. The total reaction volume of 50 µl consisted of 50 mM Tris-HCl, pH 7.4, 3.3 mM MgCl₂, 1.5 mM CTP, 1 mM Glc-1-P, and up to 15 µl of purified Bc3358. Reactions proceeded for 1 h at 30 °C. An aliquot (20 µl) was mixed with acetonitrile (40 µl) and 0.5 M ammonium acetate, pH 5.3 (2 µl), and a portion (30 µl) was chromatographed and detected by LC-ESI-MS/MS operating in the negative ion mode. Enzyme products were identified based on their retention time, the mass of their parent ion, and their mass spectral fragmentation pattern.

The activity of recombinant His₆Bc3359 (referred to herein as Bc3359 or 4,6-DH) was examined similarly as described above. To a total reaction volume of 50 µl was added 50 mM Tris-HCl, pH 7.4, CDP-Glc, and up to 15 µl of purified Bc3359. Reactions proceeded for 2 h at 30 °C followed by enzyme inactivation and extraction with 50 µl of chloroform (32). The activity of recombinant His₆Bc3360 (referred to herein as Bc3360 or C3-MetT) was examined using the reaction product of Bc3359 supplemented with 1 mM NADH, 3.3 mM MgCl₂, 1 mM SAM, and up to 15 µl of purified Bc3360 in a total volume of 25 µl. Reactions proceeded for 2 h at 22 °C. For the co-incubation assays, which included both Bc3360 and Bc3361, the enzymatic reaction product of Bc3359 was supplemented with 1 mM NADH, 1 mM NADPH, 3.3 mM MgCl₂, 1 mM SAM, 4 µl of purified Bc3360, and 4 µl of purified Bc3361 in a total volume of 25 µl. Reactions proceeded for 2 h at 30 °C. Aliquots of reactions were prepared as described previously and analyzed by HILIC LC-ESI-MS/MS.

NMR spectroscopy used to characterize the structure of products

Time-resolved NMR for the formation of CDP-4-keto-6-deoxy-Glc by recombinant Bc3359 was carried out in a final volume of 180 µl, essentially as described (24). The HPLC peaks of CDP-Glc, CDP-cillose, and CDP-cereose collected as described

Bacillus operon produces precursor for spore glycosylation

previously were lyophilized, dissolved in D₂O (99.9%), supplemented with 1 μ l of 10 mM DSS (4,4-dimethyl-4-silapentane-1-sulfonic acid), and analyzed by NMR spectroscopy (Agilent DD2 600 MHz NMR spectrometer equipped with a cryogenic 3-mm probe). Proton and carbon chemical shifts were referenced to an internal DSS peak set at 0.00 ppm for both proton and carbon spectra. The one-dimensional proton NMR spectrum was recorded using a water-presaturated pulse sequence and obtained with a spectral width of 6 kHz, a 90° pulse field angle (7.5 μ s), a 2.7-s acquisition time, and a 2-s relaxation delay. Proton chemical shifts were assigned by a COSY (correlation spectroscopy) experiment. Carbon chemical shifts as well as the connectivity between carbons and protons were determined by a heteronuclear multiple bond correlation (HMBC) experiment. The configuration of each hydroxyl group on CDP-cillose or CDP-cereose was determined by one-dimensional proton and ROESY (rotating-frame Overhauser spectroscopy) experiment. Data processing and plotting were performed using MestreNova software.

RNA isolation and RT-PCR

A 1:100 dilution of an overnight BHI culture of *B. cereus* ATCC 14579 was used to inoculate 50 ml of liquid medium (BHI or Msgg), and the cultures were grown for up to 72 h at 30 °C with shaking (200 rpm). Cells were rapidly pelleted by centrifugation (10,000 \times g for 1 min at 4 °C), resuspended in 0.8 ml of lysozyme solution (14), and incubated at room temperature for 10 min. To each sample 80 μ l of 10 \times EB (0.3 M NaOAc, pH 5.2, 50 mM EDTA, 5% Sarkosyl, and 1.42 M β -mercaptoethanol) was added. After 3 min at 65 °C, 1 volume of 70 °C preheated acidic phenol (phenol:AcE buffer: 50 mM NaOAc, pH 5.1, and 5 mM EDTA (1:1 v/v)) was added, and the mixture was incubated at 65 °C for 7 min. The sample was centrifuged (10,000 \times g for 5 min at 4 °C), and the top aqueous layer was collected and mixed with an equal volume of chloroform. Nucleic acid partitioned to the upper phase was collected, mixed with 1 volume of 30 mM NaOAc, pH 5.2, and 3 volumes of cold ethanol, and nucleic acids were precipitated at -20 °C. To digest the remnant genomic DNA, an aliquot of 5 μ g of crude RNA was treated with DNase I. The RNA was ethanol-precipitated, and a portion was used for transcript analyses by reverse transcriptase (RT) and PCR reactions. The RT reaction (20 μ l, final) consisted of 250 ng of RNA, 1 μ l of 10 μ M gene-specific reverse primers, buffer, 0.2 μ M dNTPs, and 1 unit of reverse transcriptase (SuperScript III, Invitrogen). Negative control RT reactions were done without added reverse transcriptase. Transcripts of genes in the C3CM operon, negative controls, and a positive control (SigA) were amplified, each at final 25 μ l, by PCR reaction that included 2 μ l of RT reaction, buffer, dNTPs, 1 unit of TaqDNA polymerase (Promega), and gene-specific sense and antisense primers (0.4 μ M) (primer sets TM001 and TM002 for *BC3358*, TM003 and TM004 for *BC3359*, TM005 and TM006 for *BC3360*, TM007 and TM008 for *BC3361*, and ZL347 and ZL348 for SigA) (see supplemental Table S2). Following PCR, a portion (8 μ l) of each RT-PCR reaction was loaded on a 1% agarose-TAE gel casted with 10 μ g/ml ethidium bromide, separated by gel electrophoresis, and UV-imaged using Gel Imager.

GC-MS analyses for identification of cereose and cillose

As cereose and cillose are labile sugars, mild hydrolysis was used. Purified spores collected either from liquid culture or scraped from agar plates were washed and suspended. Around 1×10^9 spores were supplemented with 10 μ g of inositol and hydrolyzed with 0.2 M TFA for 2 h at 70 °C, and the released monosaccharides were reduced to their alditols (35) and acetylated. The resulting alditol-acetate derivatives were analyzed using a GC/EI-MS system (Agilent 7890a/5975c) equipped with an autosampler injector (Agilent 7693). A 1- μ l sample was injected into the GC column (Equity-1 or DB-5, 30 m \times 0.25 mm, 0.25- μ m film thickness) using split mode (1:50) with an injector inlet setting of 250 °C (helium at 3 ml/min), and chromatography was performed as described previously (14). In some cases the GC column used was Rtx-2330 by RESTEK. MS data were collected after a solvent delay of 5 min, and the ion abundance in the range of 50 to 550 *m/z* was recorded. The spectra were analyzed using MSD ChemStation. To determine the elution time of authentic cereose and cillose and the EI-mass fragments formed, CDP-cereose and CDP-cillose were produced and purified over an HILIC column, TFA-hydrolyzed, converted to alditol acetate, separated by GC using a DB-5 column, and analyzed by EI-MS using the above GC conditions.

Mutant generation in C3CM operon

Gene knock-out was achieved by double crossover recombination as described previously (14). Two DNA fragments flanking gene *BC3360* and two DNA fragments flanking gene *BC3361* were PCR-amplified by specific primer sets ZL479 and ZL480, ZL481 and ZL482, ZL489 and ZL490, and ZL491 and ZL492, respectively (see supplemental Table S2). The flanking regions were cloned individually by primer sets ZL007 and ZL008 and ZL009 and ZL123, respectively, into the pZL-KO shuttle plasmid (14), a derivative of pBCB13 that harbors the thermosensitive ORI (origin of replication) from pMAD (37, 38). The cloning strategy for chromosomal integration at a non-permissive temperature and subsequently a double crossover recombination event was conducted as described previously (14) to achieve the resulting *B. cereus* mutant strains Δ *BC3360* and Δ *BC3361*. For complementation of mutants, PCR was used to amplify the *BC3360* and *BC3361* genomic DNA region from wild-type *B. cereus* ATCC 14579 with primer sets ZL483 and ZL484 and ZL485 and ZL486, respectively. Each DNA fragment was cloned into the pDZ vector, a derivative *E. coli*/*Bacillus* shuttle plasmid of pDG148-stu (34), which was generated by primer sets ZL213 and ZL214 as described previously (14).

Germination analysis of mutants

Spores from *B. cereus* wild-type and mutant strains Δ *BC3360* and Δ *BC3361* were prepared as stated previously. Prior to germination, the purified spores were heated at 70 °C for 30 min and washed again with ddw. Equal amounts of spores (calculated to an optical density, $A_{600} = 0.8$) were resuspended in germination solution (50 mM inosine in 10 mM Tris-HCl, pH 8, and 10 mM NaCl), and the degree of germination was monitored at A_{600} over a time course of 32 min (36).

Exosporium extraction and urea-SDS treatment

Purified spores from *B. cereus* wild type were washed twice in water, and the exosporium extraction was conducted as described previously (19). Briefly, the spores were subjected to four successive passages through a French press (20,000 p.s.i.), and the exosporium-free spores were recovered after centrifugation (3000 × g, 30 min, 4 °C). Exosporium in the supernatant was pelleted by Ultracentrifuge at 120,000 × g for 30 min at 4 °C, treated by mild acid hydrolysis, derivatized to alditol acetates, and analyzed by GC-MS.

Spores were also suspended in urea-SDS buffer (50 mM Tris-HCl, pH 7, 2% SDS, and 8 M urea) and boiled for 15 min as described (20, 21). The sample was then centrifuged at 10,000 × g for 10 min at 4 °C, and the supernatant was dialyzed against ddw and lyophilized followed by mild acid hydrolysis, alditol-acetate derivatization, and GC-MS analyses.

Author contributions—M. B. conceived and coordinated the study. Z. L. designed, performed, and analyzed most of the experiments. M. B., Z. L., and T. M. wrote the paper. T. M. performed gene expression and in-microbe experiments as well as the initial GC-MS experiments. K. B. designed and cloned the constructs and initiated the enzymology studies. S. N. and S. P. contributed to the in-microbe experiments and with A. C. contributed to the GC-MS analyses. Z. S. helped with protein purification. All authors reviewed the results and approved the final version of the manuscript.

Acknowledgment—We thank Dr. John Glushka of the Complex Carbohydrate Research Center for help with NMR spectroscopy.

References

1. Jacques, M. (1996) Role of lipo-oligosaccharides and lipopolysaccharides in bacterial adherence. *Trends Microbiol.* **4**, 408–409
2. Köhler, H., Rodrigues, S. P., and McCormick, B. A. (2002) *Shigella flexneri* interactions with the basolateral membrane domain of polarized model intestinal epithelium: role of lipopolysaccharide in cell invasion and in activation of the mitogen-activated protein kinase ERK. *Infect. Immun.* **70**, 1150–1158
3. Tang, H. B., DiMango, E., Bryan, R., Gambello, M., Iglewski, B. H., Goldberg, J. B., and Prince, A. (1996) Contribution of specific *Pseudomonas aeruginosa* virulence factors to pathogenesis of pneumonia in a neonatal mouse model of infection. *Infect. Immun.* **64**, 37–43
4. Day, C. J., Tran, E. N., Semchenko, E. A., Tram, G., Hartley-Tassell, L. E., Ng, P. S., King, R. M., Ulanovsky, R., McAtamney, S., Apicella, M. A., Tiralongo, J., Morona, R., Korolik, V., and Jennings, M. P. (2015) Glycan: glycan interactions: high affinity biomolecular interactions that can mediate binding of pathogenic bacteria to host cells. *Proc. Natl. Acad. Sci. U. S. A.* **112**, E7266–E7275
5. Cabeen, M. T., and Jacobs-Wagner, C. (2005) Bacterial cell shape. *Nat. Rev. Microbiol.* **3**, 601–610
6. Sylvestre, P., Couture-Tosi, E., and Mock, M. (2002) A collagen-like surface glycoprotein is a structural component of the *Bacillus anthracis* exosporium. *Mol. Microbiol.* **45**, 169–178
7. Steichen, C., Chen, P., Kearney, J. F., and Turnbough, C. L. (2003) Identification of the immunodominant protein and other proteins of the *Bacillus anthracis* exosporium. *J. Bacteriol.* **185**, 1903–1910
8. Daubenspeck, J. M., Zeng, H., Chen, P., Dong, S., Steichen, C. T., Krishna, N. R., Pritchard, D. G., and Turnbough, C. L., Jr. (2004) Novel oligosaccharide side chains of the collagen-like region of BclA, the major glycoprotein of the *Bacillus anthracis* exosporium. *J. Biol. Chem.* **279**, 30945–30953
9. Lequette, Y., Garénaux, E., Tauveron, G., Dumez, S., Perchat, S., Slomianny, C., Lereclus, D., Guérardel, Y., and Faille, C. (2011) Role played by

- exosporium glycoproteins in the surface properties of *Bacillus cereus* spores and in their adhesion to stainless steel. *Appl. Environ. Microbiol.* **77**, 4905–4911
10. Oliva, C. R., Swiecki, M. K., Griguer, C. E., Lisanby, M. W., Bullard, D. C., Turnbough, C. L., and Kearney, J. F. (2008) The integrin Mac-1 (CR3) mediates internalization and directs *Bacillus anthracis* spores into professional phagocytes. *Proc. Natl. Acad. Sci. U. S. A.* **105**, 1261–1266
11. Oliva, C., Turnbough, C. L., Jr., and Kearney, J. F. (2009) CD14-Mac-1 interactions in *Bacillus anthracis* spore internalization by macrophages. *Proc. Natl. Acad. Sci. U.S.A.* **106**, 13957–13962
12. Lequette, Y., Garénaux, E., Combrouse, T., Dias Tdel, L., Ronse, A., Slomianny, C., Trivelli, X., Guerardel, Y., and Faille, C. (2011) Domains of BclA, the major surface glycoprotein of the *B. cereus* exosporium: glycosylation patterns and role in spore surface properties. *Biofouling* **27**, 751–761
13. Abhyankar, W., Hossain, A. H., Djajasaputra, A., Permpoonpattana, P., Ter Beek, A., Dekker, H. L., Cutting, S. M., Brul, S., de Koning, L. J., and de Koster, C. G. (2013) In pursuit of protein targets: proteomic characterization of bacterial spore outer layers. *J. Proteome Res.* **12**, 4507–4521
14. Li, Z., Hwang, S., and Bar-Peled, M. (2016) Discovery of a unique extracellular polysaccharide in members of the pathogenic *Bacillus* that can co-form with spores. *J. Biol. Chem.* **291**, 19051–19067
15. Bruender, N. A., Thoden, J. B., Kaur, M., Avey, M. K., and Holden, H. M. (2010) Molecular architecture of a C-3'-methyltransferase involved in the biosynthesis of D-tetronitrose. *Biochemistry* **49**, 5891–5898
16. Fang, J., Zhang, Y., Huang, L., Jia, X., Zhang, Q., Zhang, X., Tang, G., and Liu, W. (2008) Cloning and characterization of the tetrocarcin A gene cluster from *Micromonospora chalcea* NRRL 11289 reveals a highly conserved strategy for tetrone biosynthesis in spiro-tetronate antibiotics. *J. Bacteriol.* **190**, 6014–6025
17. Zhang, H., White-Phillip, J. A., Melançon, C. E., 3rd, Kwon, H. J., Yu, W. L., and Liu, H. W. (2007) Elucidation of the kijanimicin gene cluster: insights into the biosynthesis of spiro-tetronate antibiotics and nitrosugars. *J. Am. Chem. Soc.* **129**, 14670–14683
18. Maes, E., Krzewinski, F., Garenaux, E., Lequette, Y., Coddeville, B., Trivelli, X., Ronse, A., Faille, C., and Guerardel, Y. (2016) Glycosylation of BclA glycoprotein from *Bacillus cereus* and *Bacillus anthracis* exosporium is domain-specific. *J. Biol. Chem.* **291**, 9666–9677
19. Faille, C., Lequette, Y., Ronse, A., Slomianny, C., Garénaux, E., and Guerardel, Y. (2010) Morphology and physico-chemical properties of *Bacillus* spores surrounded or not with an exosporium: consequences on their ability to adhere to stainless steel. *Int. J. Food Microbiol.* **143**, 125–135
20. Todd, S. J., Moir, A. J., Johnson, M. J., and Moir, A. (2003) Genes of *Bacillus cereus* and *Bacillus anthracis* encoding proteins of the exosporium. *J. Bacteriol.* **185**, 3373–3378
21. Thompson, B. M., Hsieh, H. Y., Spreng, K. A., and Stewart, G. C. (2011) The co-dependence of BxpB/ExsFA and BclA for proper incorporation into the exosporium of *Bacillus anthracis*. *Mol. Microbiol.* **79**, 799–813
22. Thompson, B. M., Waller, L. N., Fox, K. F., Fox, A., and Stewart, G. C. (2007) The BclB glycoprotein of *Bacillus anthracis* is involved in exosporium integrity. *J. Bacteriol.* **189**, 6704–6713
23. Martinez, V., Ingwers, M., Smith, J., Glushka, J., Yang, T., and Bar-Peled, M. (2012) Biosynthesis of UDP-4-keto-6-deoxyglucose and UDP-rhamnose in pathogenic fungi *Magnaporthe grisea* and *Botryotinia fuckeliana*. *J. Biol. Chem.* **287**, 879–892
24. Li, Z., Hwang, S., Ericson, J., Bowler, K., and Bar-Peled, M. (2015) Pen and Pal are nucleotide-sugar dehydratases that convert UDP-GlcNAc to UDP-6-deoxy-D-GlcNAc-5,6-ene and then to UDP-4-keto-6-deoxy-L-AltNAc for CMP-pseudaminic acid synthesis in *Bacillus thuringiensis*. *J. Biol. Chem.* **290**, 691–704
25. Hwang, S., Li, Z., Bar-Peled, Y., Aronov, A., Ericson, J., and Bar-Peled, M. (2014) The biosynthesis of UDP-D-FucNAc-4N-(2)-oxoglutarate (UDP-yelosamine) in *Bacillus cereus* ATCC 14579: Pat and Pyl, an aminotransferase and an ATP-dependent Grasp protein that ligates 2-oxoglutarate to UDP-4-amino-sugars. *J. Biol. Chem.* **289**, 35620–35632
26. Gu, X., Glushka, J., Yin, Y., Xu, Y., Denny, T., Smith, J., Jiang, Y., and Bar-Peled, M. (2010) Identification of a bifunctional UDP-4-keto-pentose/UDP-xylose synthase in the plant pathogenic bacterium *Ralstonia*

Bacillus operon produces precursor for spore glycosylation

- solanacearum* strain GMI1000, a distinct member of the 4,6-dehydratase and decarboxylase family. *J. Biol. Chem.* **285**, 9030–9040
27. Du, Y. L., Alkhalaf, L. M., and Ryan, K. S. (2015) *In vitro* reconstitution of indolmycin biosynthesis reveals the molecular basis of oxazolinone assembly. *Proc. Natl. Acad. Sci. U. S. A.* **112**, 2717–2722
 28. Barkovich, R. J., Shtanko, A., Shepherd, J. A., Lee, P. T., Myles, D. C., Tzagoloff, A., and Clarke, C. F. (1997) Characterization of the *COQ5* gene from *Saccharomyces cerevisiae*: evidence for a C-methyltransferase in ubiquinone biosynthesis. *J. Biol. Chem.* **272**, 9182–9188
 29. Thorson, J. S., Lo, S. F., and Liu, H. W. (1993) Molecular basis of 3,6-dideoxyhexose biosynthesis: elucidation of Cdp-ascarylose biosynthetic genes and their relationship to other 3,6-dideoxyhexose pathways. *J. Am. Chem. Soc.* **115**, 5827–5828
 30. Branda, S. S., González-Pastor, J. E., Ben-Yehuda, S., Losick, R., and Kolter, R. (2001) Fruiting body formation by *Bacillus subtilis*. *Proc. Natl. Acad. Sci. U. S. A.* **98**, 11621–11626
 31. Hornstra, L. M., de Vries, Y. P., de Vos, W. M., and Abee, T. (2006) Influence of sporulation medium composition on transcription of ger operons and the germination response of spores of *Bacillus cereus* ATCC 14579. *Appl. Environ. Microbiol.* **72**, 3746–3749
 32. Yang, T., Bar-Peled, L., Gebhart, L., Lee, S. G., and Bar-Peled, M. (2009) Identification of galacturonic acid-1-phosphate kinase, a new member of the GHMP kinase superfamily in plants, and comparison with galactose-1-phosphate kinase. *J. Biol. Chem.* **284**, 21526–21535
 33. Yang, T., Bar-Peled, Y., Smith, J. A., Glushka, J., and Bar-Peled, M. (2012) In-microbe formation of nucleotide sugars in engineered *Escherichia coli*. *Anal. Biochem.* **421**, 691–698
 34. Joseph, P., Fantino, J. R., Herbaud, M. L., and Denizot, F. (2001) Rapid orientated cloning in a shuttle vector allowing modulated gene expression in *Bacillus subtilis*. *FEMS Microbiol. Lett.* **205**, 91–97
 35. York, W. S., Darvill, A. G., Mcneil, M., Stevenson, T. T., and Albersheim, P. (1986) Isolation and characterization of plant-cell walls and cell-wall components. *Methods Enzymol.* **118**, 3–40
 36. Barlass, P. J., Houston, C. W., Clements, M. O., and Moir, A. (2002) Germination of *Bacillus cereus* spores in response to L-alanine and to inosine: the roles of gerL and gerQ operons. *Microbiology* **148**, 2089–2095
 37. Pereira, P. M., Veiga, H., Jorge, A. M., and Pinho, M. G. (2010) Fluorescent reporters for studies of cellular localization of proteins in *Staphylococcus aureus*. *Appl. Environ. Microbiol.* **76**, 4346–4353
 38. Arnaud, M., Chastanet, A., and Débarbouillé, M. (2004) New vector for efficient allelic replacement in naturally nontransformable, low-GC-content, Gram-positive bacteria. *Appl. Environ. Microbiol.* **70**, 6887–6891

A four-gene operon in *Bacillus cereus* produces two rare spore-decorating sugars
Zi Li, Thiya Mukherjee, Kyle Bowler, Sholeh Namdari, Zachary Snow, Sarah
Prestridge, Alexandra Carlton and Maor Bar-Peled

J. Biol. Chem. 2017, 292:7636-7650.

doi: 10.1074/jbc.M117.777417 originally published online March 15, 2017

Access the most updated version of this article at doi: [10.1074/jbc.M117.777417](https://doi.org/10.1074/jbc.M117.777417)

Alerts:

- [When this article is cited](#)
- [When a correction for this article is posted](#)

[Click here](#) to choose from all of JBC's e-mail alerts

Supplemental material:

<http://www.jbc.org/content/suppl/2017/03/15/M117.777417.DC1>

This article cites 38 references, 25 of which can be accessed free at
<http://www.jbc.org/content/292/18/7636.full.html#ref-list-1>